New Phytologist

Research

WRKY46 promotes ammonium tolerance in Arabidopsis by repressing NUDX9 and indole-3-acetic acid-conjugating genes and by inhibiting ammonium efflux in the root elongation zone

Dong-Wei Di[1], Li Sun[1,2], Meng Wang[1], Jingjing Wu[1,3], Herbert J. Kronzucker[4,5], Shuang Fang[6], Jinfang Chu[6], Weiming Shi[1] and Guangjie Li[1]

[1]State Key Laboratory of Soil and Sustainable Agriculture, Institute of Soil Science, Chinese Academy of Sciences, Nanjing 210008, China; [2]State Key Laboratory of Crop Genetics and Germplasm Enhancement, Cytogenetics Institute, Nanjing Agricultural University/Jiangsu Collaborative Innovation Center for Modern Crop Production, Nanjing, Jiangsu 210095, China; [3]Institute of Food Crops, Jiangsu Academy of Agricultural Sciences, Nanjing, Jiangsu 210014, China; [4]School of BioSciences, The University of Melbourne, Parkville, Vic. 3010, Australia; [5]Faculty of Land and Food Systems, University of British Columbia, Vancouver, BC V6T 1Z4, Canada; [6]National Centre for Plant Gene Research (Beijing), Institute of Genetics and Developmental Biology, Chinese Academy of Sciences, Beijing 100049, China

Author for correspondence:
Guangjie Li
Email: gjli@issas.ac.cn

Received: *19 May 2021*
Accepted: *8 June 2021*

New Phytologist (2021)
doi: 10.1111/nph.17554

Key words: free IAA, NH_4^+ efflux, NH_4^+ toxicity, protein N-glycosylation, root growth inhibition, WRKY46.

Summary

- Ammonium (NH_4^+) is toxic to root growth in most plants, even at moderate concentrations. Transcriptional regulation is one of the most important mechanisms in the response of plants to NH_4^+ toxicity, but the nature of the involvement of transcription factors (TFs) in this regulation remains unclear.
- Here, RNA-seq analysis was performed on Arabidopsis roots to screen for ammonium-responsive TFs. WRKY46, the member of the WRKY transcription factor family most responsive to NH_4^+, was selected. We defined the role of WRKY46 using mutation and overexpression assays, and characterized the regulation of NUDX9 and indole-3-acetic acid (IAA)-conjugating genes by WRKY46 via yeast one-hybrid and electrophoretic mobility shift assays and chromatin immunoprecipitation-quantitative real-time polymerase chain reaction (ChIP-qPCR).
- Knockout of *WRKY46* increased, while overexpression of *WRKY46* decreased, NH_4^+-suppression of the primary root. WRKY46 is shown to directly bind to the promoters of the NUDX9 and IAA-conjugating genes (*GH3.1*, *GH3.6*, *UGT75D1*, *UGT84B2*) and to inhibit their transcription, thus positively regulating free IAA content and stabilizing protein N-glycosylation, leading to an inhibition of NH_4^+ efflux in the root elongation zone (EZ).
- We identify TF involvement in the regulation of NH_4^+ efflux in the EZ, and show that WRKY46 inhibits NH_4^+ efflux by negative regulation of NUDX9 and IAA-conjugating genes.

Introduction

Ammonium (NH_4^+) is one of the principal forms of nitrogen for plants (Crawford, 1995; Kronzucker *et al.*, 1995; von Wiren *et al.*, 2000; Kronzucker *et al.*, 2001; Glass, *et al.*, 2002); however, high concentrations of NH_4^+ are typically toxic to plants, and this manifests most dramatically, and most universally, in stunted root growth (Kronzucker *et al.*, 2001; Britto & Kronzucker, 2002; Li *et al.*, 2011; Di *et al.*, 2018). Under high-NH_4^+ stress, roots are the initial site of stress perception, followed by a series of physiological, cellular, and morphological changes (Li *et al.*, 2014; Liu & von Wiren, 2017). Among these, root dysplasia, especially the inhibition of primary root (PR) growth, is a hallmark symptom of high-NH_4^+ stress (Zheng *et al.*, 2015; Straub *et al.*, 2017). Elucidation of the mechanisms by which PR growth is inhibited under an elevated NH_4^+ supply would constitute a key step in improving our understanding of the adaptation and acclimation of root system architecture to this important nutrient stress, and possibly to nutrient stresses more generally.

The mechanisms by which NH_4^+ toxicity occurs in the context of PR growth are somewhat unclear, but alterations in rhizosphere acidification, K^+ deficiency, hormone disturbance, elevated unidirectional root NH_4^+ fluxes, and decreased N-glycosylation of proteins have all been implicated (Britto & Kronzucker, 2002). As all of the hypothesized mechanisms of NH_4^+ toxicity are linked to the permeation of NH_4^+, or perhaps NH_3 (Coskun *et al.*, 2013; Munns *et al.*, 2020), into the cell, useful clues can be obtained by studying transmembrane NH_4^+ fluxes. The fact that elevated unidirectional NH_4^+ fluxes into plant roots have been linked to root growth inhibition in NH_4^+-sensitive species supplied with NH_4^+ as the sole or dominant

source of nitrogen has been well documented (Britto *et al.*, 2001a). Subsequently, a study from our laboratories showed that NH_4^+ predominantly inhibits PR growth by affecting the elongation zone (EZ) and that this is associated with elevated NH_4^+ efflux in Arabidopsis roots (Li *et al.*, 2010). However, the physiological and molecular processes underlying the elevated NH_4^+ efflux induced by high NH_4^+ concentrations are still largely unclear. In particular, the upstream regulatory factors that control the futile transmembrane NH_4^+ cycling remain unknown.

N-glycosylation is one of most common post-transcriptional protein modifications in eukaryotes, and it affects many processes, from enzyme activities to the folding, stability, and intermolecular interaction of proteins (Zeng *et al.*, 2018). In plants, N-glycosylation defects have been associated with hypersensitivity to abiotic stresses (Hoeberichts *et al.*, 2008; Maruta *et al.*, 2008; Jiao *et al.*, 2020) and, in the case of severe defects, embryo lethality (Lukowitz *et al.*, 2001). Moreover, it has been suggested that protein N-glycosylation alteration is associated with PR inhibition under high-NH_4^+ stress (Qin *et al.*, 2008; Jadid *et al.*, 2011). Three genes, GDP-mannose pyrophosphorylase (*VTC1*), GDP-D-mannose pyrophosphohydrolase (*NUDX9*), and dolichol phosphate mannose synthase 1 (*DPMS1*) have been reported to be involved in the regulation of PR growth under high NH_4^+ conditions by regulating protein N-glycosylation. VTC1 and DPMS1 mutation resulted in less N-glycosylation and higher sensitivity to NH_4^+. By contrast, a mutation in NUDX9 led to more N-glycosylation and higher tolerance to NH_4^+, indicating a positive role for protein N-glycosylation under high-NH_4^+ stress (Qin *et al.*, 2008; Barth *et al.*, 2010; Jadid *et al.*, 2011; Tanaka *et al.*, 2015). However, how protein N-glycosylation regulates NH_4^+ sensitivity is still unclear. Mutation of VTC1 has been shown to enhance root NH_4^+ efflux in the context of PR inhibition (Li *et al.*, 2010), but it is not clear whether GMPase activity or N-glycosylation plays the main role. Moreover, auxin (indole-3-acetic acid, IAA) is critical to plant growth and development, including root elongation and development, and stress responses (Di *et al.*, 2016a). Free IAA concentrations are tightly controlled by an interplay of biosynthesis, transport, and inactivation (Korasick *et al.*, 2013). Moreover, decreases in free IAA under high NH_4^+ conditions have been reported in Arabidopsis, wheat, and rice (Kudoyarova *et al.*, 1997; Li *et al.*, 2010; Tamura *et al.*, 2010; Liu *et al.*, 2013; Di *et al.*, 2018, 2021). However, whether auxin interacts with NH_4^+ efflux in roots under high-NH_4^+ stress remains unknown.

Transcription factors (TFs) play crucial roles in numerous cellular processes by controlling the transcription of genes involved (Riechmann & Ratcliffe, 2000; Han *et al.*, 2014). However, thus far, only a few TFs have been identified in the response to NH_4^+. In rice, Indeterminate Domain 10 (IDD10) has been identified as a TF that can directly bind to the promoters of the ammonium transporter *AMT1.2* and those of glutamate dehydrogenase *GDH2* (Xuan *et al.*, 2013). GmbHLHm1, another NH_4^+-responsive TF from soybean, can directly bind to the promoter of the ammonium transporter ScAMF1 in yeast (Chiasson *et al.*, 2014). However, which TF is involved in regulating NH_4^+ flux in Arabidopsis roots, and the nature of this involvement, is unknown. WRKY is a plant-specific transcription factor, and Arabidopsis contains a 74-member polygenic family. *WRKY* genes have been shown to respond to abiotic stresses (Chen *et al.*, 2009; Bakshi & Oelmüller, 2014). In higher plants, WRKY TFs, which are characterized by the presence of diagnostic WRKY domains, specifically bind to W-box sequences ((T/C)TGAC(T/C)) in the promoter region of target genes (Li *et al.*, 2018). Molecular mechanisms of stress tolerances induced by WRKY have been extensively studied but are not well understood in the context of abiotic stresses. Little is known about the interactions of WRKY proteins with target genes under NH_4^+ stress.

In the present study, we performed RNA-seq analysis on Arabidopsis roots to screen for ammonium-responsive TFs and selected WRKY46, a member of the WRKY TF family most responsive to NH_4^+, for further investigation. We defined the role of WRKY46 using mutation and overexpression assays, and characterized the regulation of *NUDX9* and IAA-conjugating genes by WRKY46 via yeast one-hybrid and electrophoretic mobility shift assays, dual-luciferase assay and chromatin immunoprecipitation-quantitative polymerase chain reaction (ChIP-qPCR). We aimed to clarify the following: first, whether NH_4^+ fluxes in primary root tips are regulated by WRKY46; second, whether protein N-glycosylation functions as a downstream process of WRKY46 action; third, whether free IAA content is linked to WRKY46-mediated NH_4^+-flux regulation under high-NH_4^+ stress; and fourth, whether there is a relationship between protein N-glycosylation and free IAA content in the regulation of NH_4^+-flux. Our results will provide novel insights into how protein N-glycosylation, free IAA content, and NH_4^+ efflux are co-regulated in response to NH_4^+ stress. These results will help us understand how plants respond to various degrees of NH_4^+ stress, and offer novel insight into how the NH_4^+ tolerance of crops could be improved.

Materials and Methods

Plant materials and growth conditions

Arabidopsis thaliana L. (Col-0) was used as the wild-type. The *wrky46* (SALK_134310C), *wrky46-1* (SAIL_1230_H01), WRKY46*ox* and *pWRKY46::WRKY46-GFP* mutants have been described previously (Hu *et al.*, 2012; Ding *et al.*, 2013). *pGH3.6::GUS*, *pUGT75D1::GUS*, *UGT75D1ox* were obtained from Prof. Catherine Bellini (Umeå University) and Prof. Bingkai Hou (Shandong University). *pGH3.1::GUS* was generated by cloning the promoter of GH3.1 (*c.* 2000 bp from ATG) into a modified *p*CAMBIA1300 binary vector, which contained a GUS gene. *pGH3.1::GUS*/WRKY46*ox*, *pGH3.6::GUS*/WRKY46*ox*, *pUGT75D1::GUS*/WRKY46*ox* were generated by crossing *pGH3.1::GUS*, *pGH3.6::GUS* or *pUGT75D1::GUS* with WRKY46*ox*. *wrky46*/*pDR5::GUS* and WRKY46*ox*/*pDR5:GUS* were generated by crossing *wrky46* or WRKY46*ox* with *pDR5::GUS*. *vtc1-1*, *nudx9* (SALK_027992 and SALK_025038C), *gh3.1* (CS100192), *gh3.6* (CS876838), *ugt84b2* (SALK_037531c) in the Col background were obtained from the Arabidopsis Biological Resource Center (ABRC) and AraShare (a nonprofit

Arabidopsis share center, http://www.arashare.cn). Seeds were cold-treated at 4°C for 48 h, and 0.1% $HgCl_2$ was used to surface-sterilize before sowing on normal medium, which was composed as follows: 2 mM KH_2PO_4, 5 mM $NaNO_3$, 2 mM $MgSO_4$, 1 mM $CaCl_2$, 0.1 mM Fe-EDTA, 50 µM H_3BO_3, 12 µM $MnSO_4$, 1 µM $ZnCl_2$, 1 µM $CuSO_4$, 0.2 µM Na_2MoO_4, 0.5 g l^{-1} MES, 1% sucrose, 1% agarose (pH 5.7). High NH_4^+ medium was created by supplementing normal medium with 15 mM $(NH_4)_2SO_4$. Germination and plant growth were carried out at 23°C ± 1°C under a 16 h : 8 h, light : dark cycle.

Phenotype analysis

For PR length measurement, 5-d-old seedlings are transferred to new media with 15 mM $(NH_4)_2SO_4$ and 5 nM IAA for another 5 d. Primary root (PR) length was determined using ImageJ software. To measure the length of the root-tip elongation zone (EZ) and the meristem zone (MZ), images were obtained using confocal laser microscopy (LSM780; Carl Zeiss). The length of the EZ was defined as the distance between the first elongated cell and the first root hair, and the length of the MZ was defined as the distance between the quiescent center (QC) and the first elongated cell.

β-glucuronidase (GUS) staining

For details of GUS staining in Arabidopsis and *Nicotiana benthamiana*, see Supporting Information Methods S1.

RNA isolation, quantitative real-time polymerase chain reaction (qRT-PCR) and sequencing

RNA was extracted using the reagent TRIzol (Sangon Biotech Co. Ltd, Shanghai, China). Reverse transcription was performed using a HiScript 1st Strand cDNA Synthesis Kit (R111-01; Vazyme Biotech Co. Ltd, Nanjing, China). One microgram of total RNA was used to synthesize the first-strand cDNA. The cDNA was diluted 20 times for real-time polymerase chain reaction (RT-PCR). For details of the qRT-PCR process, see Methods S2 and an earlier study (Di *et al.*, 2018). For RNA-seq, the methods for first-strand and double-stranded cDNA synthesis and purification, sample library construction, and differentially expressed gene (DEG) identification are described in detail elsewhere (Sun *et al.*, 2020).

Net ammonium flux measurement with the non-invasive micro-test technology (NMT) system

Net NH_4^+ fluxes were measured by NMT (Physiolyzer; Younger USA LLC, Amherst, MA, USA; see Li *et al.*, 2010). Seven-day-old seedlings were transferred to fresh media with or without 30 mM NH_4Cl and grown for 12 h before measurement. Roots were placed in basal media (0.2 mM NH_4Cl, 0.1 mM $CaCl_2$, pH 5.7) 20 min before net NH_4^+ flux measurement. The NH_4^+ fluxes of the meristem and elongation zones of roots were measured in basal media for 5 min (Li *et al.*, 2010). All measurements were carried out at Xuyue Technology Co. (Beijing, China).

Determination of indole-3-acetic acid and free ammonium content

Arabidopsis roots (200 mg, fresh weight) were ground to a fine powder in liquid nitrogen and extracted with 80% MeOH containing internal standards ($^2H_2$-IAA) at −20°C for 16 h before determination. The methods are described in detail in Methods S3 and a recent study by Di *et al.* (2021).

To ascertain NH_4^+ content, 5-d-old seedlings were transferred to fresh media with or without 15 mM $(NH_4)_2SO_4$ for another 5 d. Root samples were washed with 10 mM $CaSO_4$, and frozen in liquid nitrogen, and then extracted with 1 ml of 10 mM formic acid for the NH_4^+-content assay, using high-performance liquid chromatography (HPLC), following derivatization with *o*-phthaldialdehyde (Sun *et al.*, 2020).

Chromatin immunoprecipitation-quantitative polymerase chain reaction analysis

Four-week-old *pWRKY46::WRKY46-GFP* plants were harvested and cross-linked with 1% formaldehyde. Chromatin immunoprecipitation was carried out using an antibody against green fluorescent protein (GFP; ab290, Abcam, Cambridge, UK). Input samples and immunoprecipitated samples were analyzed using qPCR. Primer sequences are listed in Table S1. The ChIP-qPCR results were normalized to the input samples. Relative enrichment was calculated as follows: Fold Enrichment = (%(ChIP/Input))/(%(Negative control/Input)).

Yeast one-hybrid (Y1H) assay

The Y1H assay was performed using a Matchmaker Gold Yeast One-Hybrid Library Screening System (Clontech, San Francisco, CA, USA). For details of the Y1H assay, see Methods S4.

Electrophoretic mobility shift assay (EMSA)

cDNA of *WRKY46* was introduced into *p*ET32a, and recombinant His-WRKY46 was purified using the Ni-NTA His Bind purification Kit (Novagen, Madison, WI, USA) according to the manufacturer's instructions. The EMSA was performed using the Lightshift Chemiluminescent EMSA Kit (Thermo Scientific, Merelbeke, Belgium). For biotin-labeled-probe (wild-type: probe-w and mutant: probe-m; Zoonbio Biotechnology, Nanjing, China) sequences, see Table S1. Unlabeled competitors (wild-type and mutant) were added in 100-fold excess.

Transient luciferase activity assay

The *WRKY46* coding sequence was introduced into *p*GreenII-062SK and constructed as *35S::WRKY46*. The *NUDX9* promoter sequence was introduced into the *p*GreenII0800-LUC vector. These two plasmids were transferred into *N. benthamiana*. Firefly luciferase (LUC) and Renilla luciferase (REN) activity were measured using the Dual-Luciferase Reporter Assay Kit (DL101-01; Vazyme Biotech Co. Ltd).

Western blotting

For concentration experiments, 10-d-old seedlings were treated with varying concentrations of $(NH_4)_2SO_4$ (0, 7.5, 15, 30 mM) for 6 h before nuclear protein extraction. For time-course experiments, 8-d-old seedlings were treated with 15 mM $(NH_4)_2SO_4$ for different durations (30, 60, 120, 240 min) before nuclear protein extraction. For auxin experiments, 5-d-old seedlings were transferred to fresh media with 5 nM IAA or 1.5 µM L-kynurenine (Kyn) for another 5 d, and were then used for nuclear protein extraction. Proteins were detected by Western blotting using a mouse anti-GFP primary antibody (1 : 1000; Abcam) and subsequently with a Sheep Anti-Rabbit IgG H&L (HRP) conjugated antibody (1 : 5000; Abcam). Anti-Histone H3 was used as a control. Protein abundance was analyzed using ImageJ software. The extent of mature N-glycoproteins in seedlings was examined using anti-horseradish peroxidase (HRP, 1 : 200 000; Sigma-Aldrich) and measurements were performed by Jingjie PTMBiolab Co. Ltd (Hangzhou, China).

Statistical analysis

Data were analyzed using Prism 6 software (GraphPad Software, https://www.graphpad.com/). Comparisons between multiple groups were conducted using two-way ANOVA tests.

Results

WRKY46 is involved in the response to high ammonium concentrations in Arabidopsis roots

To investigate the transcriptional regulation of NH_4^+ inhibition of PR growth, we first performed RNA-seq analysis for roots treated with or without NH_4^+, and > 100 TFs were implicated (Di *et al.*, 2021; Table S2). Of these, 11 members, namely *WRKY8*, *31*, *38*, *41*, *43*, *45*, *46*, *51*, *62*, *63* and *70*, belong to the same gene family, the WRKY TF family (Fig. 1a). The qRT-PCR analysis confirmed that the *WRKY*s, except for *WRKY41* and *WRKY45*, exhibited similar patterns, while *WRKY46* was the most abundantly expressed and induced by high NH_4^+ concentrations in roots (Fig. 1b).

Due to the fact that it exhibited the highest level of induction under high NH_4^+ conditions, *WRKY46* was chosen for further mechanistic examination. We monitored the *WRKY46* root expression pattern and found that *pWRKY46::GUS* was mainly confined to the root-tip elongation zone (EZ), and not the meristem zone (MZ), under control conditions; however, *pWRKY46::GUS* was much more pronounced in the EZ and MZ under high NH_4^+ conditions than under control conditions, showing that NH_4^+ induces *WRKY46* expression in the root-tip zone (Fig. 1c). Consistently, with increased treatment time and NH_4^+ concentration, WRKY46 protein levels were also strikingly enhanced (Fig. 1d,e). Overall, WRKY46 was upregulated by high NH_4^+ concentrations in roots, especially in the root-tip zone.

The knockout mutant *wrky46* and the overexpression line WRKY46*ox* were used to examine the role of WRKY46 in PR growth regulation. When grown on media with high NH_4^+ concentrations, PR length in WRKY46*ox* was significantly higher than in Col, whereas the *wrky46* mutant was more sensitive (Fig. S1). We further analyzed EZ and MZ length in Col, *wrky46*, and WRKY46*ox* (Fig. 2a,b). There was no significant difference in relative MZ length between them; however, relative EZ length was 53.5%, 41.5%, and 65.6% in Col, *wrky46*, and WRKY46*ox*, respectively, suggesting that WRKY46 mainly functions in the EZ (Fig. 2b). To confirm the high-NH_4^+-sensitive phenotype resulting from the *WRKY46* mutation, we then tested another T-DNA insertion line, *wrky46-1* (SAIL_1230_H01) (Ding *et al.*, 2013), and found that it exhibited a similar sensitivity phenotype to *wrky46* when exposed to high-NH_4^+ stress (Fig. S2). These results suggest that WRKY46 plays a positive role in protection of PR growth under high NH_4^+ conditions.

WRKY46 negatively regulates ammonium efflux in the elongation zone

Previous studies have shown that increased NH_4^+ flux at the EZ is one of the key characteristics associated with PR growth inhibition under NH_4^+ stress. As WRKY46 was mainly expressed in the EZ and positively regulated EZ growth, we asked whether WRKY46 promotion of PR growth under high NH_4^+ conditions was associated with NH_4^+-flux regulation. We therefore measured NH_4^+ net fluxes at the MZ and EZ of Col, *wrky46*, and WRKY46*ox*. Under high NH_4^+ conditions, NH_4^+ efflux increased in both MZ and EZ of the three genotypes, and the increase at the MZ of *wrky46* (120.6%) was slightly higher, while that in WRKY46*ox* (73.5%) was lower than in Col (100.5%) (Fig. 3a,c). Net NH_4^+ efflux in the EZ of Col was 166.608 pmol $cm^{-2}\,s^{-1}$, while it was enhanced to 280.895 pmol $cm^{-2}\,s^{-1}$ in *wrky46* but suppressed to 86.170 pmol $cm^{-2}\,s^{-1}$ in WRKY46*ox* (Fig. 3b,c), showing that WRKY46 indeed negatively regulates EZ NH_4^+ fluxes.

To test whether altered NH_4^+ fluxes are linked to NH_4^+ assimilation in roots, we measured free NH_4^+ contents in Col, *wrky46*, and WRKY46*ox*. However, under both control and high NH_4^+ conditions, NH_4^+ content was not different between genotypes (Fig. 3d). These results indicate that NH_4^+-flux alterations in *wrky46* and WRKY46*ox* are not linked to NH_4^+ assimilation in roots.

NUDX9, not *VTC1*, is the direct downstream gene of WRKY46

Previous studies have shown that VTC1 participates in the regulation of NH_4^+ efflux at the root EZ (Li *et al.*, 2010). To test whether *VTC1* is the downstream target of WRKY46, we analyzed *VTC1* transcription in WRKY46*ox* roots, which showed similar relative *VTC1* transcription to Col plants (Fig. 4a). The qRT-PCR data show that *VTC1* is not induced by high NH_4^+ concentrations in either Col or *wrky46*, and that the mutation in *WRKY46* also does not influence the transcription of *VTC1* (Fig. 4b), suggesting that *VTC1* is not the downstream target gene of WRKY46.

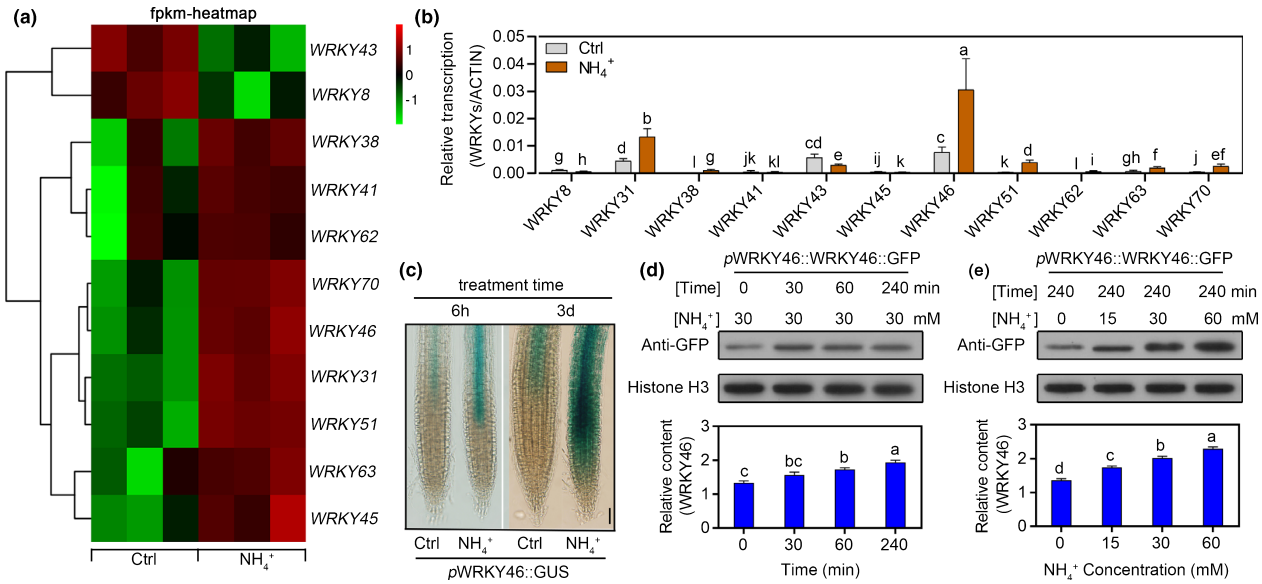

Fig. 1 WRKY transcription factors are involved in the response to high-ammonium (NH_4^+) stress. (a) Heatmap of WRKYs, created from RNA-seq data. Five-day-old Arabidopsis Columbia-0 (Col) seedlings were transferred to fresh media with or without 30 mM NH_4^+ (supplied as 15 mM $(NH_4)_2SO_4$) and grown for another 5 d, after which the roots were collected for RNA-seq analysis ($P < 0.05$). (b) Quantitative real-time polymerase chain reaction (qRT-PCR) analysis of selected *WRKY*s in response to high NH_4^+ concentrations. Five-day-old Col seedlings were transferred to fresh media with or without 30 mM NH_4^+ and grown for another 5 d, after which the roots were collected for RNA extraction and qRT-PCR analysis. Data shown are the means ± SD ($n = 3$). Error bars with different letters represent statistically significant differences ($P < 0.05$, Duncan's test). (c) β-glucuronidase (GUS) staining of *pWRKY46::GUS*. Five-day-old seedlings with *pWRKY46::GUS* were transferred to fresh media with or without 30 mM NH_4^+ for 6 h or 3 d before staining. (d) WRKY46 protein levels of roots grown on media with 30 mM NH_4^+ for different treatment times (0, 30, 60 and 240 min), and (e) grown on media with different concentrations of NH_4^+ (0, 15, 30 and 60 mM). Ten-day-old seedlings were treated and nuclear proteins were collected for Western blot experiments. Values shown are the means ± SD. Error bars with different letters represent statistically significant differences ($P < 0.05$, Duncan's test).

NUDX9 and DPMS1/2/3 are also involved in protein N-glycosylation and NH_4^+ hypersensitivity in Arabidopsis (Jadid *et al.*, 2011; Tanaka *et al.*, 2015) (Figs S3, S4). To identify the potential downstream genes of WRKY46, we determined the transcription level of these genes. The relative transcription levels of *DPMS1*, *2* and *3* were similar in both WRKY46*ox* and Col; however, *NUDX9* transcripts were 31.1% lower in WRKY46*ox* compared to Col (Figs 4c, S3c). In addition, when the high NH_4^+ condition was introduced, *NUDX9* expression increased 5.39-fold and 1.29-fold in *wrky46* and Col, respectively, compared to their counterparts under control conditions (Fig. 4d). These results suggest that WRKY46 negatively regulates *NUDX9* transcription.

To investigate whether *NUDX9* functions as the downstream target of WRKY46, we performed a ChIP-qPCR assay using *pWRKY46::WRKY46-GFP*. The enrichment of specific primers (P1–P2) in the immunoprecipitate was determined using qPCR, by tracking ChIP with an anti-GFP antibody, and the exon of *NUDX9* was used as a negative control (Fig. 4e). The two primers were significantly enriched in the immunoprecipitate (Fig. 4f). In addition, the Y1H and EMSA assays showed that WRKY46 can directly bind to the *NUDX9* promoter (Fig. 4g,h). To further test the transcriptional activity of WRKY46, we constructed a dual-luciferase (LUC) reporter plastid encoding the LUC gene driven by the *NUDX9* promoter (0–1927 bp) and a Renilla luciferase (REN) gene driven by the 35S promoter (Fig. 4i,j). We found that overexpression of WRKY46 suppresses *c.* 65% of the LUC activity compared to the vector control (Fig. 4j). These results suggest that WRKY46 can directly bind to the *NUDX9* promoter and inhibit its transcription.

WRKY46 inhibits ammonium efflux via protein N-glycosylation that stabilizes NUDX9

To gain a better understanding of the genetic relationship between *WRKY46* and *NUDX9*, we generated *wrky46/nudx9* and WRKY46*ox/nudx9* double mutants. Measurement of the of the MZ and EZ lengths found no significant difference in relative MZ length among Col, *wrky46*, WRKY46*ox*, *nudx9*, *wrky46/nudx9*, and WRKY46*ox/nudx9* under high NH_4^+ conditions (Fig. 5a). However, relative EZ length in Col, *wrky46*, WRKY46*ox*, *nudx9*, *wrky46/nudx9*, and WRKY46*ox/nudx9* was 53.7%, 42.1%, 64.9%, 67.8%, 60.3% and 76.8% (Fig. 5b), respectively.

In order to identify whether WRKY46 is involved in regulating protein N-glycosylation, the N-glycosylation levels in seedlings were checked using a specific N-glycosylation peroxidase antibody, which directly binds to the oligomannose chains

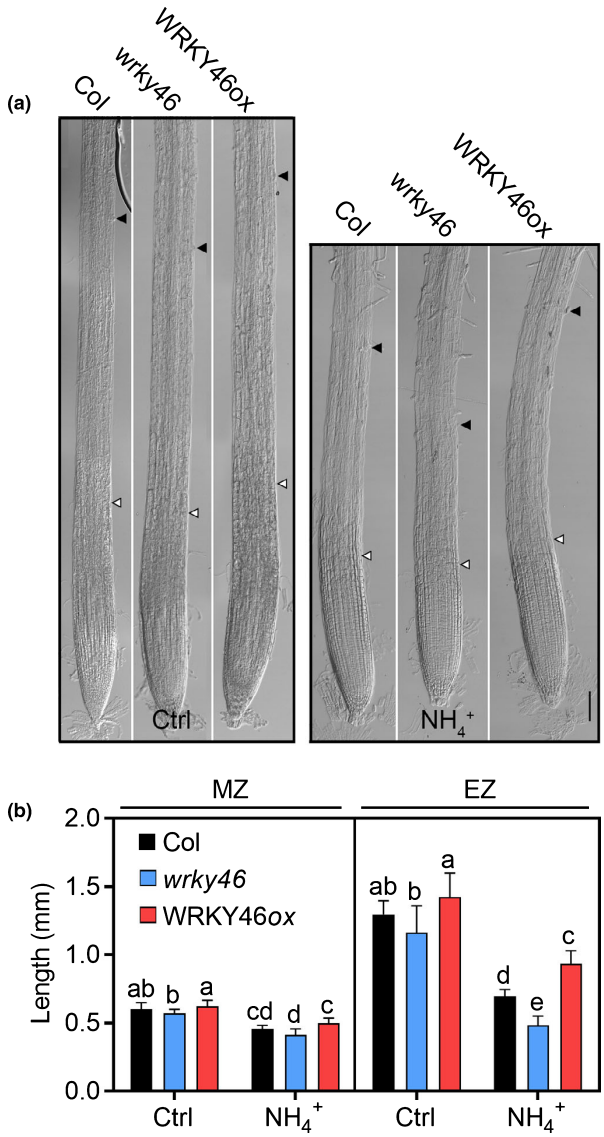

Fig. 2 WRKY46 is involved in the response to high-ammonium (NH_4^+) stress. (a) The elongation zone (EZ) of Arabidopsis Columbia-0 (Col), *wrky46*, and WRKY46*ox* seedlings. Five-day-old untreated seedlings were transferred to a medium with 0 mM or 15 mM $(NH_4)_2SO_4$, then grown for 5 d prior to observation. The interval between the two arrows indicates the EZ in the three materials (Bar, 100 μm). (b) Measurement of the length of the meristem zone (MZ) and elongation zone in Col, *wrky46*, and WRKY46*ox* seedlings. Five-day-old untreated seedlings were transferred to a medium with 0 mM or 15 mM $(NH_4)_2SO_4$, then grown for 5 d before measurement. Values shown are the means ± SD with $n = 20$. Error bars with different letters represent statistically significant differences ($P < 0.05$, Duncan's test).

of N-glycoproteins (Strasser *et al.*, 2004). Compared to Col, the *wrky46* mutant contains less N-glycoprotein, whereas WRKY46*ox* and *nudx9* contain more N-glycoprotein under control conditions, further supporting the positive role of WRKY46 in stabilizing protein N-glycosylation (Figs 5c, S5).

To test whether WRKY46 regulates NH_4^+ efflux via NUDX9-dependent N-glycosylation, we measured root NH_4^+ fluxes in *nudx9*, *wrky46/nudx9*, WRKY46*ox/nudx9*, and Col. Under high NH_4^+ conditions, NH_4^+ efflux in the MZ of *nudx9* was 78.071 pmol cm^{-2} s^{-1}, significantly lower than in Col (154.205 pmol cm^{-2} s^{-1}), but decreased to 60.335 pmol cm^{-2} s^{-1} in WRKY46*ox/nudx9* and increased to 118.509 pmol cm^{-2} s^{-1} in the *wrky46/nudx9* double mutant (Fig. 6a,b). NH_4^+ efflux under high NH_4^+ conditions in the EZ of the *nudx9* mutant was 44.3% of that in the Col; NH_4^+ efflux was increased in crosses of *wrky46* and *nudx9*, while NH_4^+ efflux was decreased to 34.9% of the level in Col in crosses of WRKY46*ox* with *nudx9* (Fig. 6d). Together with an earlier report of NH_4^+ efflux increases in the *vtc1-1* mutant (Li *et al.*, 2010), the present data confirm the positive regulatory role of protein N-glycosylation in the process of NH_4^+ efflux in roots. Furthermore, the WRKY46*ox/nudx9* double mutant had greater EZ growth and less NH_4^+ efflux than either parent under high-NH_4^+ stress, indicating that other genes are involved in the WRKY46-dependent high-NH_4^+ response and that *NUDX9* may not be the sole downstream target of WRKY46.

Indole-3-acetic acid regulators *GH3.1*, *GH3.6*, *UGT75D1*, and *UGT84B2* are direct downstream targets of WRKY46

Primary root growth inhibition under high NH_4^+ conditions is connected to IAA, and WRKY46 is involved in regulating root IAA content under osmotic/salt stress (Li *et al.*, 2010; Liu *et al.*, 2013; Ding *et al.*, 2015; Di *et al.*, 2018). Here, *NUDX9* is shown not to be the sole target of WRKY46 in regulating PR growth and NH_4^+ efflux. To test whether altered sensitivity to high NH_4^+ concentrations in *wrky46* and WRKY46*ox* is related to IAA content, we conducted GUS staining in Col/*pDR5::GUS*, *wrky46/pDR5::GUS*, and WRKY46*ox/pDR5::GUS*. After switching to high NH_4^+ media, *wrky46/pDR5::GUS* and WRKY46*ox/pDR5::GUS* displayed stronger and weaker GUS staining, respectively, compared to Col/*pDR5::GUS* (Fig. 7a). Furthermore, adding low IAA concentrations to high NH_4^+ media more effectively rescued PR growth in *wrky46* than in Col and WRKY46*ox* (Fig. S6). The results suggest that the differential sensitivity to NH_4^+ in *wrky46* and WRKY46*ox* is connected to free root IAA content. To identify how WRKY46 regulates IAA content, we first analyzed the transcription levels of auxin-conjugating genes in WRKY46*ox*. Our results show a decrease in *GH3.1*, *GH3.6*, *UGT75D1*, and *UGT84B2* in WRKY46*ox* compared to Col (Figs 7b, S7). Transcription of the IAA-conjugating genes was induced by NH_4^+ (Fig. 7c), and induction was more pronounced in the *wrky46* mutant, indicating that WRKY46 participates in the response of these genes to high NH_4^+ concentrations as a transcription inhibitor. Furthermore, MZ length in *gh3.6* and UGT75D1*ox* was sensitive and tolerant to NH_4^+, respectively, compared to Col, and the results were similar in *gh3.1* and *ugt84b2* (Fig. 7d). Interestingly, EZ growth in all mutants, *gh3.1*, *gh3.6*, *ugt84b2* was less sensitive than in Col, and in the overexpression line UGT75D1*ox* EZ growth was more sensitive than in Col (Fig. 7e). These results suggest that the transcription of genes

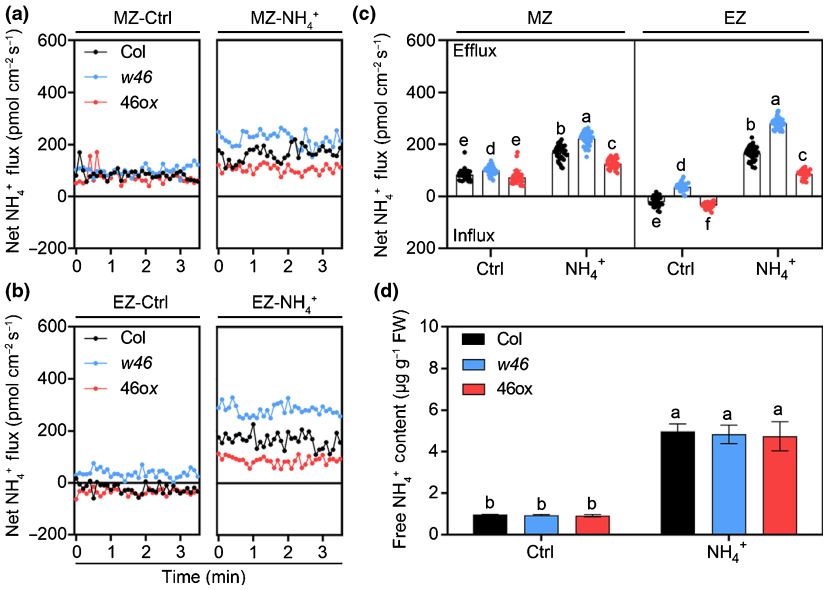

Fig. 3 WRKY46 negatively regulates ammonium (NH_4^+) fluxes in roots, especially at the elongation zone. Ammonium fluxes of Arabidopsis Columbia-0 (Col), *wrky46* (*w46*), and WRKY46*ox* (46*ox*) in the meristem zone (MZ) (a) and elongation zone (EZ) (b) of roots grown on control and NH_4^+ media. (c) Mean NH_4^+ flux in (a) and (b). Values shown are the means ± SD ($n \geq 6$). (d) Free NH_4^+ content in Col, *wrky46*, and WRKY46*ox* plants. Values shown are the means ± SD ($n = 9$). Error bars with different letters represent statistically significant differences ($P < 0.05$, Duncan's test).

encoding IAA-conjugating proteins is involved in PR growth regulation under high NH_4^+ conditions.

There are multiple W-boxes ((T)TGACT/C) in the promoters of *GH3.1*, *UGT75D1*, and *UGT84B2* (Ding *et al.*, 2015). We also found that the promoter of *GH3.6* was enriched in W-boxes (Fig. 8a). We further performed ChIP and Y1H analyses, and found that the DNA fragments amplified by the primers (P3–P10) are significantly enriched in the immunoprecipitate compared to their negative controls and that WRKY46-AD can physically bind to the promoters of *GH3.1*, *GH3.6*, *UGT75D1* and *UGT84B2* (Fig. 8b,c). To investigate this regulation *in vivo*, we then introduced *pGH3.1::GUS*, *pGH3.6::GUS*, and *pUGT75D1::GUS* into WRKY46*ox* (*pUGT84B2::GUS* did not yield a successful construct), and found that GUS was decreased in the WRKY46*ox* background, especially at the EZ, compared to Col (Fig. 8d). These results suggest that WRKY46 negatively regulates transcription of these IAA-conjugating genes by directly binding to the *GH3.1*, *GH3.6*, *UGT75D1*, and *UGT84B2* promoters. To verify the function of WRKY46 in IAA homeostasis under high NH_4^+ conditions, we measured the concentrations of free IAA and IAA conjugates (IAA-Asp and IAA-Glu). Compared to Col, the *wrky46* mutant plants consistently exhibited a greater reduction in free IAA and a higher accumulation of IAA conjugates after high NH_4^+ treatment, but a smaller decline in free IAA and a smaller accumulation of IAA conjugates were found in WRKY46*ox* (Fig. 9). The results indicate that WRKY46 positively regulates IAA content under high NH_4^+ concentrations via inhibition of the conversion of free IAA to IAA conjugates.

Free indole-3-acetic acid is involved in WRKY46-mediated inhibition of ammonium efflux in the elongation zone

To further investigate the relationship between IAA and WRKY46 regulation of NH_4^+ fluxes, we measured NH_4^+ fluxes in high NH_4^+ media with a low concentration of exogenous IAA (5 nM). When adding a low IAA dose to the high NH_4^+ medium, NH_4^+ flux decreased to similar levels in Col and *wrky46* in the MZ (Fig. 10a,b). Similarly, NH_4^+ efflux in the EZ of Col and *wrky46* grown on high NH_4^+ media also decreased after the addition of a low dose of IAA (Fig. 10c,d). Indole-3-acetic acid had a more noticeable effect in *wrky46* (Fig. 10b,d), suggesting that an IAA-dependent pathway is also involved in WRKY46 regulation of NH_4^+ flux.

To further ascertain the function of IAA in relation to NH_4^+ fluxes, we then directly measured NH_4^+ fluxes in *gh3.6* (with elevated free IAA) and UGT75D1*ox* (with reduced free IAA). The *gh3.6* exhibited lower, and UGT75D1*ox* higher, NH_4^+ efflux than Col in the EZ following high NH_4^+ treatment (Fig. 10c,d). Similarly, NH_4^+ efflux in the MZ was inhibited in *gh3.6* but promoted in UGT75D1*ox*, compared to Col, under high NH_4^+ conditions (Fig. 10a,b). Meanwhile, when exogenous IAA was added to the growth media, NH_4^+ efflux in the MZ and EZ of UGT75D1*ox* decreased to a level similar to that of Col. These data indicate that IAA mainly inhibits root NH_4^+ efflux in the EZ, and that WRKY46 is involved in this process via regulation of IAA accumulation.

Protein N-glycosylation-inhibited ammonium efflux partially depends on indole-3-acetic acid content

An earlier study reported that VTC1 is involved in regulating IAA content under high NH_4^+ conditions (Barth *et al.*, 2010). To investigate the relationship between protein N-glycosylation and free IAA, we generated *vtc1-1/pDR5::GUS* and *nudx9/pDR5::GUS*. *vtc1-1/pDR5::GUS* exhibits relatively weak staining under high NH_4^+ conditions, while *nudx9/pDR5::GUS* exhibits strong staining, compared to Col (Fig. 11a), suggesting that protein N-glycosylation is required to maintain free IAA under high NH_4^+ conditions.

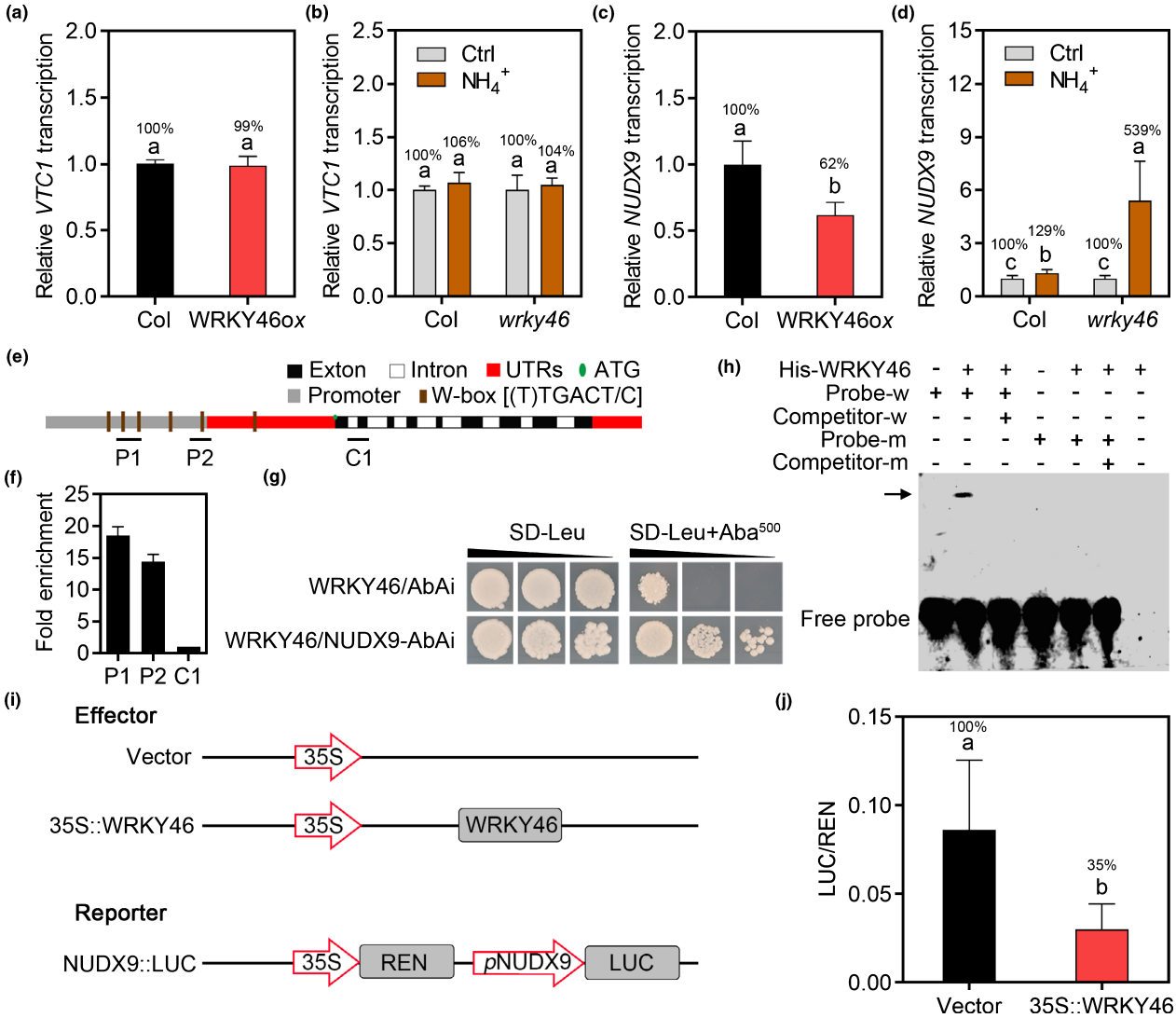

Fig. 4 *NUDX9* functions as the downstream target of WRKY46. (a, c) The relative transcription of *VTC1* (a) and *NUDX9* (c) in WRKY46*ox* plants; RNA was extracted from 10-d-old Arabidopsis Columbia-0 (Col) and WRKY46*ox* seedling roots. Data are the means of three replicates. Error bars indicate ± SD; the transcription level of *VTC1* and *NUDX9* in Col were normalized as 1. (b, d) The relative transcription of *VTC1* (b) and *NUDX9* (d) in Col and *wrkyw46* after high NH_4^+ treatment. Ten-day-old seedlings were treated with 15 mM $(NH_4)_2SO_4$ for 4 h before roots were collected for RNA extraction. Data are the means of three replicates. Error bars with different letters represent statistically significant differences ($P < 0.05$, Duncan's test). (e) Schematic diagrams of the *NUDX9* promoter showing potential WRKY46-binding sites. Translational start sites are shown as ATG. (f) Fold enrichment of *NUDX9* by WRKY46. Segment C1 located in the coding region was used as a negative control. An input sample was used to normalize the qualitative polymerase chain reaction (qPCR) results for each ChIP sample. Fold enrichment is presented as the ratio of normalized results from P1 ~ P2 and control. Data are the means ± SD. (g) Yeast one-hybrid (Y1H) assays showing WRKY46 physically binding to the *NUDX9* promoter. Yeast expression plasmids *p*GADT7-WRKY46 were reintroduced into the yeast strain Y1H Gold carrying the reporter gene *AbAr* under the control of the *NUDX9* promoter. Transformants were screened for their growth on the yeast synthetic defined medium (SD/–Leu) in the presence of 500 ng ml^{-1} Aureobasidin A (AbA), which is used for stringent selection. The vector *p*GADT7-WRKY46 was included as a negative control. Yeast cultures were diluted (1 : 10 successive dilution series) and spotted onto plates. (h) Electrophoretic mobility shift assay (EMSA) showing that WRKY46 binds the W-box motif of the *NUDX9* promoter *in vitro*. (i, j) WRKY46 inhibits the promoter of *NUDX9* in *Nicotiana benthamiana* as demonstrated via dual-luciferase assays. The LUC : REN ratio indicates the effect of the activity of WRKY46 on the expression level of *NUDX9*. LUC: firefly luciferase activity; REN: Renilla luciferase activity. Data are means ± SD ($n = 9$). Error bars with different letters represent statistically significant differences ($P < 0.05$, Duncan's test).

To further examine the role of IAA in NH_4^+ efflux in relation to N-glycosylation, we measured NH_4^+ flux in *vtc1-1* grown on a high NH_4^+ medium with the addition of IAA, and in *nudx9* on high a NH_4^+ medium with the addition of Kyn (an IAA biosynthesis inhibitor; He *et al.*, 2011). Consistent with a previous report (Li *et al.*, 2010), NH_4^+ efflux in the MZ and EZ of *vtc1-1* increased more than in Col under high NH_4^+ treatment (Figs 10, 11b–d). However, when exogenous IAA was added to

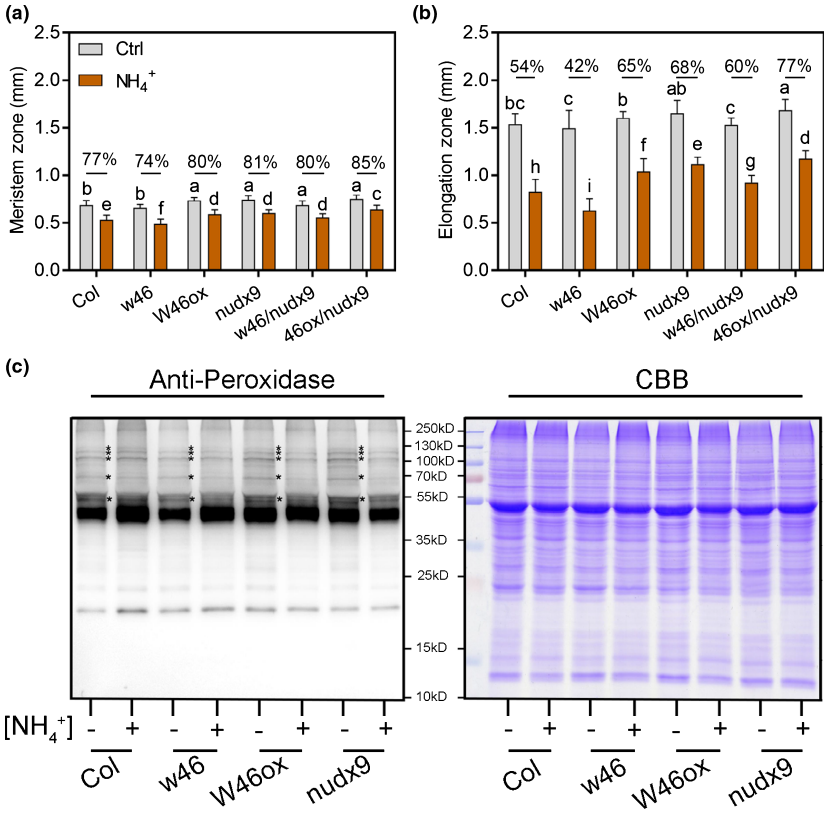

Fig. 5 WRKY46 regulates protein N-glycosylation in a NUDX9-dependent pathway. (a, b) Measurement of the length of the meristem zone (MZ) and elongation zone (EZ) in Arabidopsis Columbia-0 (Col), *nudx9*, *wrky46/nudx9* (*w46/nudx9*), and WRKY46*ox/nudx9* (46*ox/nudx9*) seedlings. Five-day-old untreated seedlings were transferred to a medium with 0 mM or 15 mM $(NH_4)_2SO_4$, then grown for 5 d before measurement. Values shown are the means ± SD with $n = 20$. Error bars with different letters represent statistically significant differences ($P < 0.05$, Duncan's test). (c) Protein N-glycosylation levels in Col, *wrky46*, *WRKY46ox* and *nudx9* plants were evaluated using a ConA-peroxidase reagent, the reaction with which is a characteristic feature of N-glycans. Coomassie Brilliant Blue (CBB) staining of protein gels was used to control for protein loading. The asterisks (*) indicate different specific N-glycoprotein bands.

high NH_4^+ media, NH_4^+ efflux in the MZ and EZ of Col and *vtc1-1* decreased to, 26.371 pmol cm^{-2} s^{-1}/79.685 pmol cm^{-2} s^{-1} and 116.944 pmol cm^{-2} s^{-1}/184.278 pmol cm^{-2} s^{-1} compared to plants grown on high NH_4^+ media, suggesting that VTC1-dependent NH_4^+ efflux is partially dependent on free IAA content (Figs 10, 11b–d). By contrast, exogenous Kyn increased NH_4^+ flux in the MZ and EZ (Fig. 11b–d). These results suggest that N-glycosylation-dependent NH_4^+ fluxes partially depend on root IAA content.

Discussion

It is well known that NH_4^+ toxicity inhibits PR growth, and the root-tip zone is the principal target. Defective protein N-glycosylation (Qin *et al.*, 2008) and elevated NH_4^+ efflux (Britto *et al.*, 2001a; Li *et al.*, 2010) at the root tip are two mechanisms linked to PR NH_4^+ sensitivity, but the underlying genetic regulation is unknown. Here, we present a genetic regulatory factor, WRKY46, that affects both N-glycosylation and NH_4^+ efflux and protects PR growth under NH_4^+ toxicity. WRKY46 supports root tolerance to NH_4^+ via direct negative regulation of *NUDX9*, which, in turn, controls protein N-glycosylation and is associated with NH_4^+ efflux suppression in the EZ. Both processes partially depend on free root IAA, and WRKY46 is shown to directly bind to the promoters of IAA-conjugating genes (*GH3.1*, *GH3.6*, *UGT75D1*, *UGT84B2*), inhibiting their transcription and thus positively regulating free IAA content, inhibiting NH_4^+ efflux, and protecting PR growth.

WRKY46 is a direct negative regulator of NUDX9, stabilizing protein N-glycosylation and reducing NH_4^+ efflux in the elongation zone

Excessive NH_4^+ efflux from roots has been shown to be strongly associated with NH_4^+ toxicity in numerous plants (Britto *et al.*, 2001b), and NH_4^+ efflux is most pronounced in the EZ and is linked to PR inhibition (Li *et al.*, 2010). However, it remained unclear which regulatory genes are involved. Here, we identify WRKY46 as a TF involved in regulating NH_4^+ fluxes in the root EZ. The results show that a lack of/overexpression of WRKY46 can significantly increase/decrease root NH_4^+ efflux in the EZ under high NH_4^+ conditions (Fig. 3a–c). In addition, our results showed that osmotic/salt stress also induced the expression of WRKY46 in roots, but only slightly altered the PR growth sensitivity to osmotic/salt stress (Fig. S8).

In previous work, a link was established between NH_4^+ efflux, root sensitivity, and VTC1 (Qin *et al.*, 2008; Barth *et al.*, 2010; Kempinski *et al.*, 2011). We first speculated as to whether *VTC1* is a downstream target of WRKY46, and analyzed *VTC1* transcription in *wrky46* and WRKY46*ox*. Qin *et al.* (2008) suggested that *VTC1* transcriptional and protein levels are not affected by NH_4^+, and our data show that the transcriptional level of *VTC1*

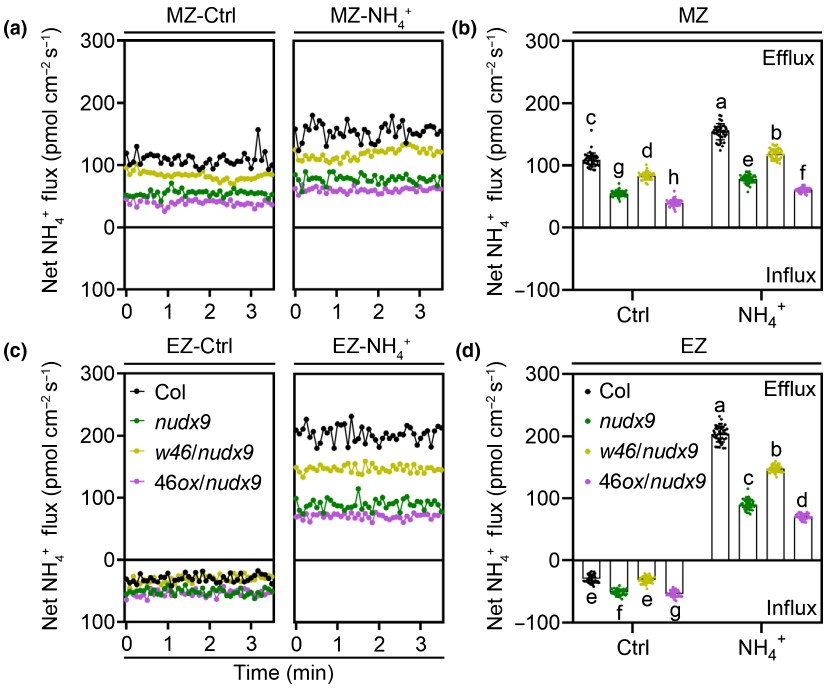

Fig. 6 WRKY46 regulates NH_4^+ fluxes in a NUDX9-dependent pathway. (a, c) NH_4^+ flux in Arabidopsis Columbia-0 (Col), *nudx9*, *wrky46/nudx9* (*w46/nudx9*), and WRKY46*ox*/*nudx9* (46*ox*/*nudx9*) in the meristem zone (MZ) (a) and elongation zone (EZ) (c) of roots grown on control and NH_4^+ media. (b) Mean NH_4^+ flux in (a). (d) Mean NH_4^+ flux in (c). Values shown are the means ± SD ($n \geq 6$). Error bars with different letters represent statistically significant differences ($P < 0.05$, Duncan's test).

is not regulated by either NH_4^+ or WRKY46, indicating that *VTC1* is not the downstream gene of WRKY46 (Fig. 4a,b). Two additional enzymes, NUDX9 and DPMS1, have also been reported to participate in the response to high NH_4^+ concentrations in the context of protein N-glycosylation (Jadid *et al.*, 2011; Tanaka *et al.*, 2015). A mutation in the *NUDX9* gene resulted in improved N-glycosylation and higher NH_4^+ tolerance (Tanaka *et al.*, 2015; Liu & von Wiren, 2017). Knockout of DPMS1 led to less N-glycosylation and higher NH_4^+ sensitivity (Jadid *et al.*, 2011). The results presented here show that the transcription of *NUDX9*, but not *DPMS1-3*, is inhibited in WRKY46*ox* compared to Col (Figs 4c, S3c). Furthermore, our data show that WRKY46 directly binds to the W-box of the promoter of *NUDX9* and functions as a repressor of *NUDX9* in regulating NH_4^+ sensitivity, as revealed by ChIP-qPCR, Y1H, dual-luciferase assay, and EMSA. Previous promoter deletion analysis of GS1.2 showed that the necessary DNA region for the NH_4^+ response contains Dof, bHLH, and WRKY-binding domains (Konishi *et al.*, 2017). To clarify whether the W-box is responsible/necessary for the NH_4^+ response, we directly synthesized the promoters of *GH3.1* and *UGT75D1* without W-boxes (Fig. S9a), introduced these promoters into the *p*BI121::GUS vector and transferred the recombinant plastids into *N. benthamiana*. We found that high-NH_4^+ stress strengthens GUS staining in both the wild-type and mutant promoter::GUS of *GH3.1* and *UGT75D1*, suggesting that the W-box might not be the key motif for the high-NH_4^+ response (Fig. S9b).

Impaired N-glycosylation results in the accumulation of unfolded or misfolded proteins and activation of the UPR-signaling pathway, followed by increased protein folding activity and cell death (Ron & Walter, 2007; Qin *et al.*, 2008). However, the key regulatory elements controlling N-glycosylation during NH_4^+ exposure remained unidentified. Only one other report suggested that N-glycosylation may be related to NH_4^+ efflux (Li *et al.*, 2010). Here, we provide strong genetic evidence that N-glycosylation does indeed regulate root NH_4^+ efflux under high NH_4^+ conditions using the *nudx9* mutant (Figs 5c,d, 6). To examine the role of NUDX9 in WRKY46-dependent NH_4^+ efflux, we measured NH_4^+ fluxes in *wrky46 nudx9* and WRKY46*ox nudx9*, and the data support the notion that NUDX9 is located downstream of WRKY46 in the genetic cascade of NH_4^+ efflux regulation (Figs 3, 6). In agreement with these results, N-glycoprotein levels were decreased in *wrky46* but increased in WRKY46*ox* under control conditions (Fig. 5c). However, the N-glycoprotein content was dramatically decreased in *nudx9* and WRKY46*ox* upon high-NH_4^+ treatment, suggesting that the high-NH_4^+-induced N-glycoprotein accumulation depends on NUDX9, but that high NH_4^+ concentrations can also decrease N-glycoprotein levels in *nudx9* and WRKY46*ox* via another pathway, similar to the trend in abscisic acid (ABA) accumulation observed under high-NH_4^+ stress in the *amos1* mutant (Li *et al.*, 2012; Fig. 5c). These data, together with the findings from previous studies, indicate that N-glycosylation plays a central and positive role in protecting PR growth under high NH_4^+ conditions, downregulating NH_4^+ efflux. Molecular evidence, genetic analysis, and electrophysiological data support the finding that a NUDX9-dependent N-glycosylation pathway is involved in WRKY46-regulated NH_4^+ flux.

Interestingly, Kempinski *et al.* (2011) found that the two mutants *pmi-1* and *pmm-12*, which function upstream of VTC1 and contribute to GMPase activity, grown on high NH_4^+ media exhibited unchanged PR growth from their

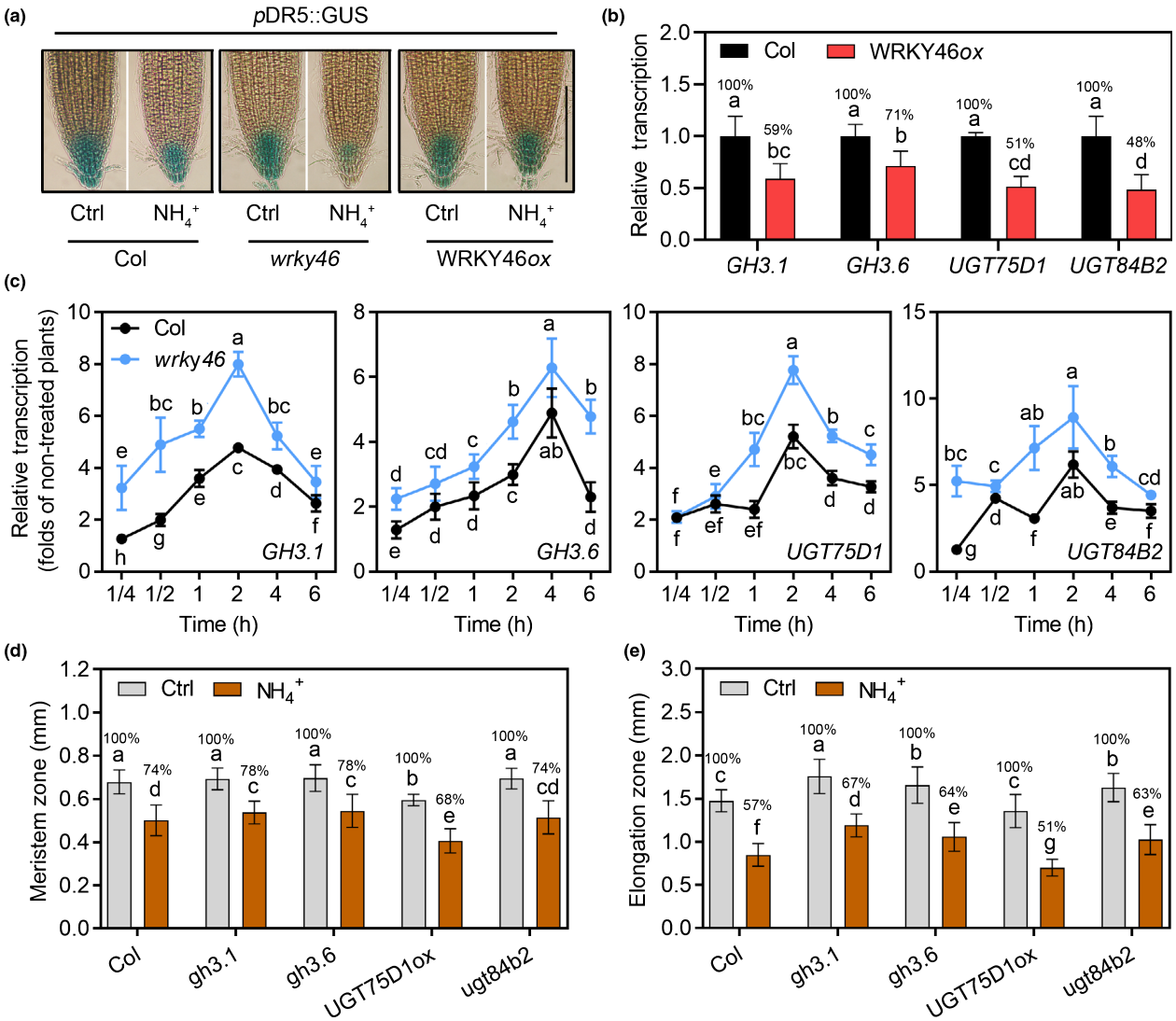

Fig. 7 WRKY46 regulation of primary root growth under high-NH_4^+ stress is associated with indole-3-acetic acid (IAA) accumulation in roots. (a) *pDR5::GUS* staining in Arabidopsis Col/*pDR5::GUS*, *wrky46*/*pDR5::GUS*, and WRKY46*ox*/*pDR5::GUS* grown on media with or without 30 mM NH_4^+. Five-day-old seedlings were transferred to media with or without 15 mM $(NH_4)_2SO_4$ for another 3 d before β-glucuronidase (GUS) staining. Bar, 0.5 mm. (b) Fold enrichment graph showing downregulated transcription of *GH3.1*, *GH3.6*, *UGT75D1* and *UGT84B2* in WRKY46*ox* plants. RNA was extracted from 10-d-old Col and WRKY46*ox* seedling roots. Data are the means of three replicates. Error bars indicate ± SD. (c) NH_4^+-induced transcription of IAA-conjugating genes revealed by quantitative real-time polymerase chain reaction (qRT-PCR) assays. Ten-day-old seedlings were treated with 15 mM $(NH_4)_2SO_4$ for various periods of time before roots were collected for RNA extraction. Data are the means of three replicates. Error bars indicate ± SD. (d, e) Measurement of the length of the meristem zone (MZ) (d) and elongation zone (EZ) (e) in Col, *gh3.1*, *gh3.6*, UGT75D1*ox* and *ugt84b2* seedlings. Five-day-old untreated seedlings were transferred to a medium with 0 mM or 15 mM $(NH_4)_2SO_4$, then grown for 5 d before measurement. Values shown are the means ± SD with $n = 20$. Error bars with different letters represent statistically significant differences ($P < 0.05$, Duncan's test).

wild-type control plants. Here, we present additional evidence to show that N-glycosylation, but not GMPase, is involved in regulating root NH_4^+ efflux and PR growth sensitivity: First, the *nudx9* and *dmps1* mutants, which are affected in N-glycosylation but not GMPase, exhibit altered NH_4^+ sensitivity and efflux in roots. Overexpression of *WRKY46*, by contrast, resulted in more N-glycosylation of proteins and higher NH_4^+ tolerance, and knockout of *DMPS1* led to reduced N-glycosylation and higher NH_4^+ sensitivity. Second, IAA, which is linked to H^+-ATPase function, decreased strongly in *vtc1-1* (Shen *et al.*, 2006; Barth *et al.*, 2010; Tanaka *et al.*, 2015; Wang *et al.*, 2016), but *nudx9* accumulated more free IAA under high NH_4^+ conditions (Fig. 11a). In addition, N-glycoproteome profiling has shown that N-glycosylation

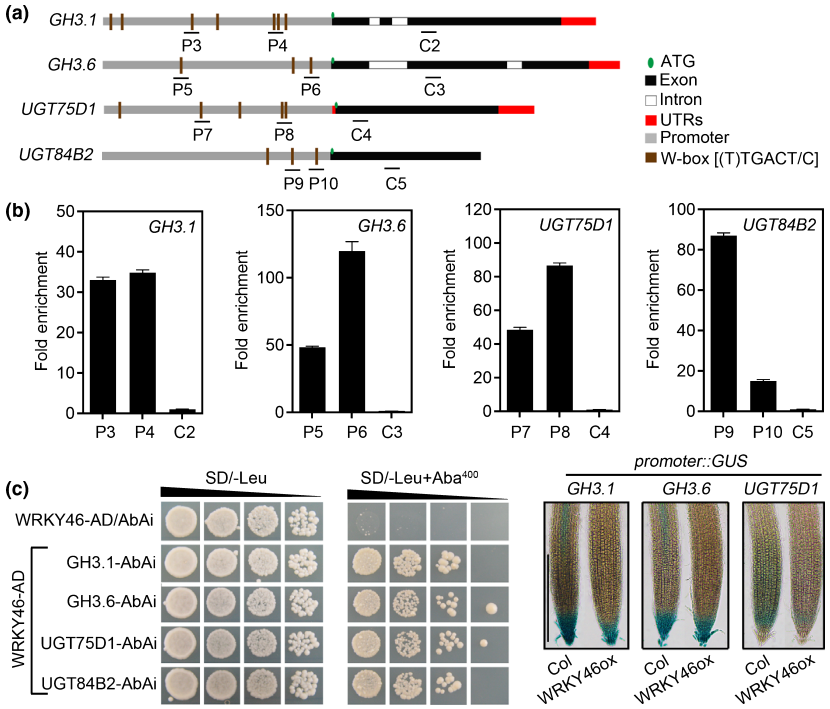

Fig. 8 WRKY46 directly binds to the promoters of *GH3.1*, *GH3.6*, *UGT75D1*, and *UGT84B2* in Arabidopsis. (a) Schematic diagrams of *GH3.1*, *GH3.6*, *UGT75D1* and *UGT84B2* promoters showing potential WRKY46-binding sites. Translational start sites are shown as ATG. (b) Fold enrichment of IAA-conjugating genes by WRKY46. Segment C located in the coding region was used as a negative control. An input sample was used to normalize the quantitative polymerase chain reaction (qPCR) results for each ChIP sample. Fold enrichment is presented as the ratio of normalized results from P3 ~ P10 and control. Data are the means ± SD. (c) Yeast one-hybrid (Y1H) assays showing WRKY46 physically binding to the *GH3.1*, *GH3.6*, *UGT75D*, and *UGT84B2* promoters. *p*GADT7-WRKY46 yeast expression plasmids were reintroduced into the yeast strain Y1H Gold carrying the reporter gene *AbAr* under the control of the *GH3.1*, *GH3.6*, *UGT75D1*, and *UGT84B2* promoters. Transformants were screened for their growth on yeast synthetic defined medium (SD/–Leu) in the presence of 400 ng ml^{-1}AbA, used for stringent selection. The empty vector *p*GADT7 was included as a negative control. Yeast cultures were diluted (1 : 10 successive dilution series) and spotted onto plates. (d) β-glucuronidase (GUS) staining of *pGH3.1::GUS*, *pGH3.6::GUS* and *pUGT75D1::GUS* in *WRKY46ox* plants. Five-day-old seedlings were transferred to fresh media for another 3 d before GUS staining. Bar, 1 mm.

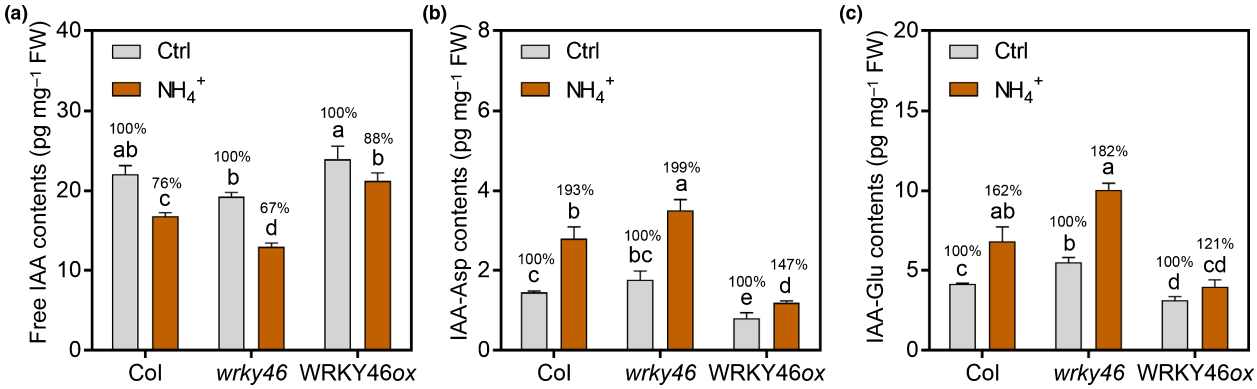

Fig. 9 Indole-3-acetic acid (IAA) conjugates and free IAA content in Col, *wrky46*, and WRKY46*ox* roots. (a) Free IAA content, (b) IAA-Asp content, and (c) IAA-Glu content in Arabidopsis Columbia-0 (Col), *wrky46*, and *WRKY46ox* roots. Root samples were prepared from 5-d-old seedlings with or without 30 mM NH_4^+ treatment for 5 d. Three biological repeats were carried out per treatment. Values shown are the means ± SD. Error bars with different letters represent statistically significant differences ($P < 0.05$, Duncan's test).

modification is found in key enzymes involved in IAA homeostasis (Ruiz-May *et al.*, 2014; Zeng *et al.*, 2018). Third, *nudx9* and WRKY46*ox* (with high N-glycosylation levels) exhibit decreased NH_4^+ efflux, and *wrky46* and *vtc1-1* (with low N-glycosylation levels) exhibit increased NH_4^+ efflux compared to Col (Figs 3, 6, 11b–d).

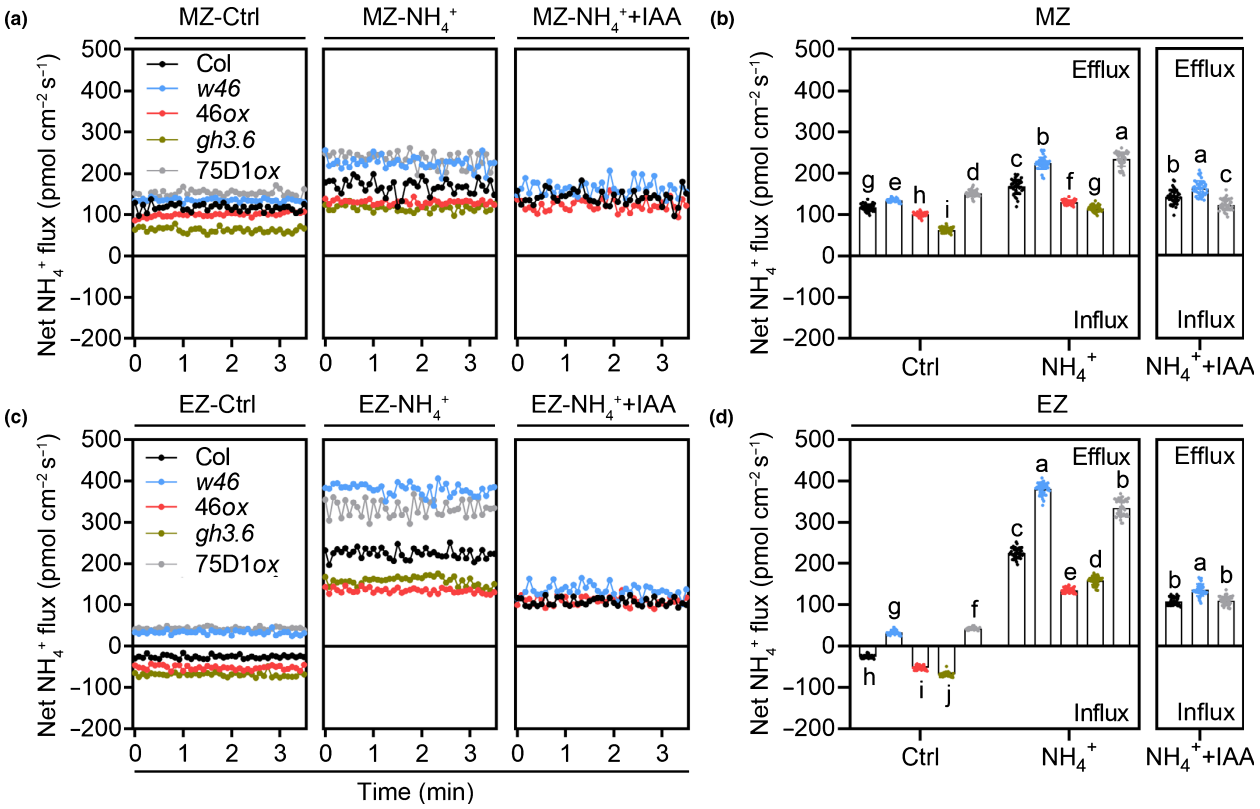

Fig. 10 WRKY46 is involved in regulating NH_4^+ fluxes in the elongation zone of roots under high-NH_4^+ stress. (a, c) NH_4^+ flux of Arabidopsis Columbia-0 (Col), *wrky46* (*w46*), WRKY46*ox* (46*ox*), *gh3.6*, and UGT75D1*ox* (75D1*ox*) in the meristem zone (MZ) (a) and elongation zone (EZ) (c) of roots grown on control, NH_4^+, and NH_4^++IAA media. (b) Mean NH_4^+ flux in (a). (d) Mean NH_4^+ flux in (c). Values shown are the means ± SD ($n \geq 6$). Error bars with different letters represent statistically significant differences ($P < 0.05$, Duncan's test).

Free indole-3-acetic acid functions downstream in protein N-glycosylation to regulate ammonium efflux

A recent study suggested that high-NH_4^+ stress decreases free IAA content via the acceleration of IAA conjugation rather than the inhibition of IAA biosynthesis in the EZ of roots (Di *et al.*, 2021). Here, we demonstrate that WRKY46 functions as a TF that mainly inhibits the transcription of IAA-conjugating genes *GH3.1*, *GH3.6*, *UGT75D1* and *UGT84B2* in the EZ of roots and inhibits the high-NH_4^+-induced IAA conjugation in roots (Figs 7–9). Interestingly, the aforementioned study reported that excess NH_4^+ decreased free IAA and increased IAA-Asp in rice roots, and that the increase in IAA-Asp was repressed by the mutation of OsNADH-GOGAT1, suggesting a tight connection between NH_4^+ assimilation and IAA conjugation in roots under high-NH_4^+ stress (Tamura *et al.*, 2010). These results indicate that high-NH_4^+ stress impacts IAA homeostasis at two critical levels: WRKY46-dependent transcriptional regulation and NADH-GOGAT1-dependent metabolic regulation. Furthermore, our recent study showed that neither mutation nor overexpression of *WRKY46* influences NH_4^+ metabolism, indicating that the WRKY46-dependent transcriptional regulation of IAA conjugation is not connected to NH_4^+ assimilation (Fig. 3d). However, we cannot, at this point, clarify whether NADH-GOGAT-dependent amino acid metabolism plays a role in WRKY46-dependent transcriptional regulation of IAA homeostasis under high-NH_4^+ stress. In addition, considering that tryptophan is the main precursor of IAA biosynthesis (Bartel, 1997; Di *et al.*, 2016b), it will be important, in future work, to investigate the connection between amino acid metabolism and IAA homeostasis under high-NH_4^+ stress.

The results of a previous study and our *pDR5::GUS* staining analysis in *vtc1-1* and *nudx9* suggest that N-glycosylation might also positively regulate free IAA in roots under high NH_4^+ conditions (Barth *et al.*, 2010). We therefore employed pharmacological and genetic approaches to examine the link between free IAA and NH_4^+ flux. Our data show that the addition of exogenous IAA decreases NH_4^+ efflux in *vtc1-1* and the addition of exogenous Kyn increases NH_4^+ efflux in *nudx9*. This indicates that N-glycosylation inhibits NH_4^+ efflux under high NH_4^+ conditions, and that this is at least in part dependent on free IAA content (Fig. 11b–d). A recent study reported that N-glycosylation can increase protein stability in response to pathogen attack (Xia *et al.*, 2020). Furthermore, N-glycoproteome profiling showed that key enzymes involved in IAA homeostasis (e.g. IAA-amino acid hydrolase ILR1 and

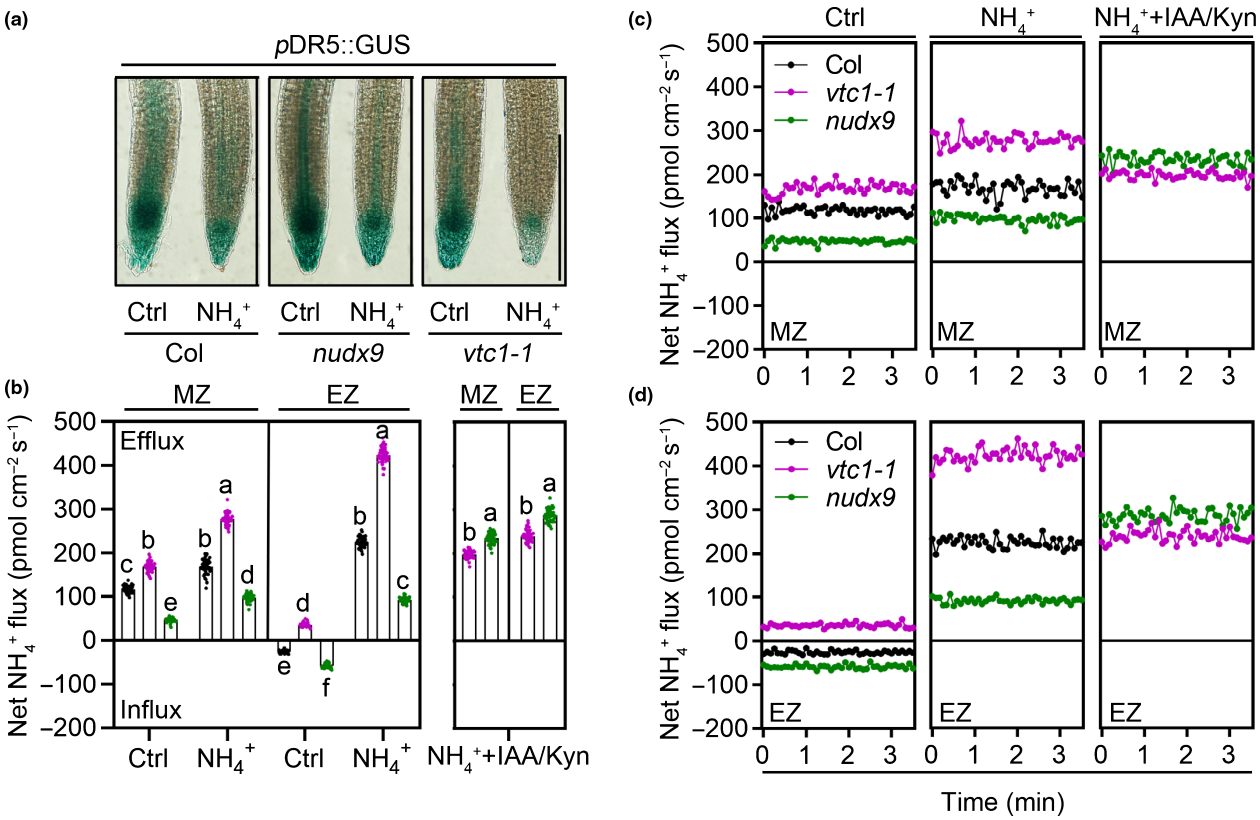

Fig. 11 Protein N-glycosylation and NH_4^+ flux partially depend on indole-3-acetic acid (IAA) content. (a) *pDR5::GUS* staining in Arabidopsis Col/*pDR5::GUS*, *nudx9*/*pDR5::GUS*, and *vtc1-1*/*pDR5::GUS* grown on media with or without 30 mM NH_4^+. Five-day-old seedlings were transferred to media with or without 15 mM $(NH_4)_2SO_4$ for another 3 d before GUS staining. Bar, 1 mm. (b) Mean NH_4^+ flux in the meristem zone (MZ) and elongation zone (EZ) of *vtc1-1* and *nudx9* roots grown on control, NH_4^+, NH_4^++IAA (*vtc1-1*), and NH_4^++L-kynurenine (Kyn) (*nudx9*). (c, d) NH_4^+ flux in *vtc1-1* and *nudx9* in the MZ (c) and EZ (d) of roots grown on control, NH_4^+, NH_4^++IAA (*vtc1-1*), and NH_4^++Kyn (*nudx9*) media. Values shown are the means ± SD ($n \geq 6$). Error bars with different letters represent statistically significant differences ($P < 0.05$, Duncan's test).

β-glucosidase BG1) are N-glycoproteins, whose involvement in salt and drought stresses has been shown (Ruiz-May *et al.*, 2014; Zeng *et al.*, 2018; Jiao *et al.*, 2020). We concluded that some IAA conjugate hydrolases may be modified by N-glycosylation under high NH_4^+ conditions and that the N-glycosylated enzymes exhibit enhanced protein stability in hydrolyzing IAA conjugates, leading to higher levels of free IAA.

Indole-3-acetic acid stimulation of PR growth has been investigated in numerous studies, and there are two theories to explain how auxin promotes root growth: the 'acid-growth theory' and the 'gene expression theory' (Rayle *et al.*, 1970; Takahashi *et al.*, 2012; Enders & Strader, 2015; Wang *et al.*, 2016; Yin *et al.*, 2020). Here, we demonstrate that free IAA can suppress NH_4^+ efflux in roots under high NH_4^+ (Fig. 10). Our data show that mutants with low endogenous IAA, *wrky46*, *vtc1-1*, and UGT75D1*ox*, exhibit higher NH_4^+ efflux and less PR elongation compared to Col (Figs 2, 3, 10, 11). However, addition of IAA to media could restore NH_4^+ efflux in the same genotypes grown on high NH_4^+ media to Col levels (Fig. 10). Consistent with this, NH_4^+ efflux of the mutants with high endogenous IAA (e.g. WRKY46*ox*, *nudx9* and *gh3.6*) was lower than in Col grown on a high NH_4^+ medium (Fig. 10). By contrast, the *nudx9* mutant grown on a high NH_4^+ medium with Kyn (an IAA biosynthesis inhibitor) exhibited increased NH_4^+ efflux compared to that on a high NH_4^+ medium (Fig. 11b–d). One explanation for how free IAA regulates NH_4^+ efflux may relate to H^+ balance. There are two possible mechanisms: firstly, IAA exists in two forms, IAAH and IAA^-; the former can pass plasma membranes freely by simple diffusion without requiring a transporter or energy consumption, while the latter crosses plasma membranes by active transport mediated by AUXIN1/LIKE AUX1 (AUX/LAX), PIN-FORMED (PIN) and P-Glyco-Protein/Multi-Drug Resistance (PGP/MDR) proteins, and this step requires energy (Ren & Lin, 2014; Adamowski & Friml, 2015; Swarup & Bhosale, 2019). Different ratios of IAA^- : IAAH transport between cells and the rhizosphere will result in more or less H^+ retention in cells, and then more or less NH_4^+ efflux (Michniewicz *et al.*, 2007); secondly, IAA has been shown to regulate the phosphorylation of H^+-ATPase under aluminum stress, and it is therefore also possible that IAA influences H^+ balance by directly regulating the

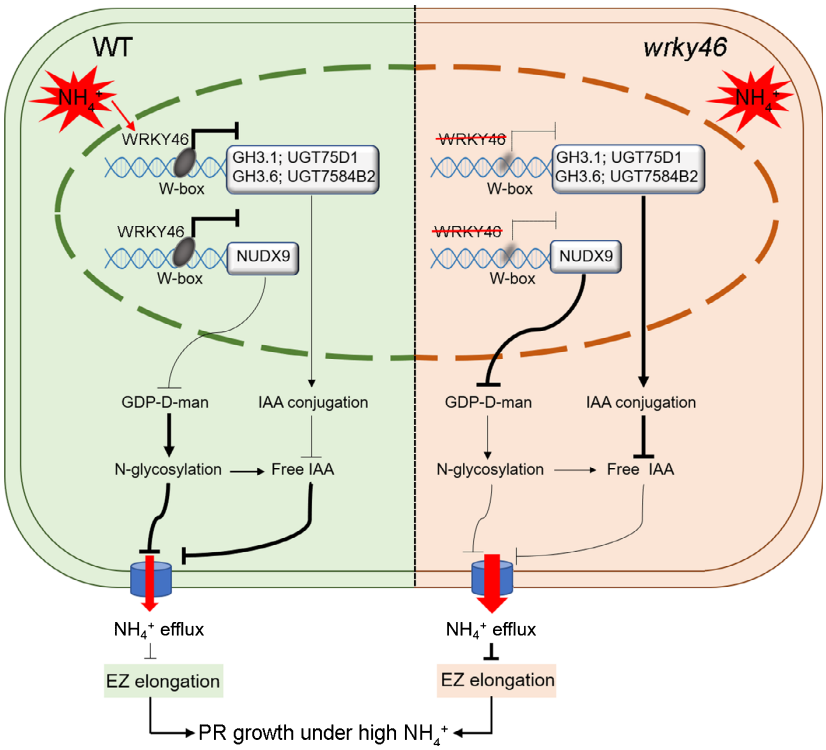

Fig. 12 A working model for WRKY46 function under high-NH_4^+ stress. Under high NH_4^+ conditions, NH_4^+ induces the expression of the transcription factor WRKY46 in Arabidopsis. Subsequently, WRKY46 directly binds to the promoters of *GH3.1*, *GH3.6*, *UGT75D1* and *UGT84B2* and inhibits their transcription, thereby maintaining free indole-3-acetic acid (IAA) content and primary root (PR) growth. WRKY46 further inhibits the transcription of NUDX9 and stabilizes protein N-glycosylation levels. As a result, IAA-biosynthetic enzymes maintain stability after N-glycosylation, increasing IAA biosynthesis under high NH_4^+ conditions. Elevated free IAA induces the transcription of IAA-conjugating genes, a process which is linked indirectly to the inhibition of *WRKY46* transcription. Overall, WRKY46 maintains IAA homeostasis by inhibiting IAA conjugation and protein N-glycosylation. Black arrows indicate positive functions. Black bars indicate negative functions. Red arrows indicate the NH_4^+ efflux. The width of the arrows and bars represents the physiological processes becoming stronger or weaker. EZ, elongation zone.

activity of H^+-ATPase through phosphorylation modification (Shen *et al.*, 2006; Takahashi *et al.*, 2012; Wang *et al.*, 2016). Alternatively, as our data also show that exogenous IAA could not completely inhibit the NH_4^+ efflux induced by knockdown of *VTC1* (Fig. 11), we infer there may has a direct inhibition of N-glycosylation of regulatory domains on the NH_4^+-efflux transporter or channel, preventing closure. As the molecular identity of the NH_4^+-efflux transporter is not yet known, this cannot as yet be tested more directly. Based on our present evidence, however, free IAA clearly functions to inhibit NH_4^+ efflux under both normal and high NH_4^+ conditions.

In conclusion, we propose that the regulation of protein N-glycosylation and free IAA by WRKY46 might function as a protective mechanism under NH_4^+ stress. High NH_4^+ concentrations induce WRKY46 expression, and WRKY46 accumulation negatively regulates the transcription of *NUDX9* and IAA-conjugating genes. As a result, more protein N-glycosylation, higher free IAA, and reduced NH_4^+ efflux occur in roots (Fig. 12). However, when NH_4^+ stress becomes weak or disappears, the accumulation of free IAA negatively regulates the expression of WRKY46 and positively regulates IAA-conjugating genes to maintain IAA content in roots within narrow limits (Figs 6, S10). Moreover, WRKY46 functions as an auxin stabilizer under high NH_4^+ conditions and helps maintain relatively stable free IAA concentrations in roots. Our results provide novel insight into how protein N-glycosylation, free IAA, and NH_4^+ efflux are co-regulated in response to NH_4^+ stress. In brief, WRKY46 could be a valuable genetic resource with which to develop high-NH_4^+-tolerant crop cultivars, and the insight into the interaction of protein N-glycosylation, free IAA, and NH_4^+ efflux under high NH_4^+ conditions offers a novel clue to how NH_4^+ tolerance in plants could be improved.

Acknowledgements

We thank Prof. Guang-Qin Guo (Lanzhou University, China), Prof. Shaojian Zheng (Zhejiang University, China), Prof. Diqiu Yu (Chinese Academy of Sciences, China), Prof. Catherine Bellini, and Prof. Bingkai Hou for kindly providing transgenic seeds, and the Arabidopsis Biological Resource Center of Ohio State University and AraShare for mutant seeds. We thank Yue Xu and Yunqi Liu (Zhongguancun Xuyue Non-invasive Microtest Technology Industrial Alliance) for technical advice on net NH_4^+ flux measurements. This work was supported by grants from the National Natural Science Foundation of China (31430095 and 31601823), the Natural Science Foundation of Jiangsu Province (no. BK20200050) and the University of Melbourne.

Author contributions

D-WD, GL and WS planned and designed the research; D-WD, LS, MW and JW performed the research and analyzed the data; SF and JC determined IAA concentrations; D-WD, MW, GL, WS and HJK wrote the paper. All authors approved the manuscript.

ORCID

Dong-Wei Di https://orcid.org/0000-0003-4453-6862
Herbert J. Kronzucker https://orcid.org/0000-0002-9358-0029
Guangjie Li https://orcid.org/0000-0003-4603-6722
Weiming Shi https://orcid.org/0000-0002-6055-0704
Li Sun https://orcid.org/0000-0002-3718-163X
Meng Wang https://orcid.org/0000-0002-7773-0998

References

Adamowski M, Friml J. 2015. PIN-dependent auxin transport: action, regulation, and evolution. *Plant Cell* **27**: 20–32.

Bakshi M, Oelmüller R. 2014. WRKY transcription factors: Jack of many trades in plants. *Plant Signaling and Behavior* **9**: e27700.

Bartel B. 1997. Auxin biosynthesis. *Annual Review of Plant Physiology and Plant Molecular Biology* **48**: 51–66.

Barth C, Gouzd ZA, Steele HP, Imperio RM. 2010. A mutation in GDP-mannose pyrophosphorylase causes conditional hypersensitivity to ammonium, resulting in Arabidopsis root growth inhibition, altered ammonium metabolism, and hormone homeostasis. *Journal of Experimental Botany* **61**: 379–394.

Britto DT, Glass AD, Kronzucker HJ, Siddiqi MY. 2001a. Cytosolic concentrations and transmembrane fluxes of NH_4^+/NH_3. An evaluation of recent proposals. *Plant Physiology* **125**: 523–526.

Britto DT, Kronzucker HJ. 2002. NH_4^+ toxicity in higher plants: a critical review. *Journal of Plant Physiology* **159**: 567–584.

Britto DT, Siddiqi MY, Glass AD, Kronzucker HJ. 2001b. Futile transmembrane NH_4^+ cycling: a cellular hypothesis to explain ammonium toxicity in plants. *Proceedings of the National Academy of Sciences, USA* **98**: 4255–4258.

Chen YF, Li LQ, Xu Q, Kong YH, Wang H, Wu WH. 2009. The WRKY6 transcription factor modulates PHOSPHATE1 expression in response to low Pi stress in Arabidopsis. *Plant Cell* **21**: 3554–3566.

Chiasson DM, Loughlin PC, Mazurkiewicz D, Mohammadidehcheshmeh M, Fedorova EE, Okamoto M, McLean E, Glass AD, Smith SE, Bisseling T *et al.* 2014. Soybean *SAT1* (*Symbiotic Ammonium Transporter 1*) encodes a bHLH transcription factor involved in nodule growth and NH_4^+ transport. *Proceedings of the National Academy of Sciences, USA* **111**: 4814–4819.

Coskun D, Britto DT, Li M, Becker A, Kronzucker HJ. 2013. Rapid ammonia gas transport accounts for futile transmembrane cycling under NH_3/NH_4^+ toxicity in plant roots. *Plant Physiology* **163**: 1859–1867.

Crawford NM. 1995. Nitrate - nutrient and signal for plant growth. *Plant Cell* **7**: 859–868.

Di DW, Li G, Sun L, Wu J, Wang M, Kronzucker HJ, Fang S, Chu J, Shi W. 2021. High ammonium inhibits root growth in *Arabidopsis thaliana* by promoting auxin conjugation rather than inhibiting auxin biosynthesis. *Journal of Plant Physiology* **261**: 153415.

Di DW, Sun L, Zhang XN, Li GJ, Kronzucker HJ, Shi W. 2018. Involvement of auxin in the regulation of ammonium tolerance in rice (*Oryza sativa* L.). *Plant and Soil* **432**: 373–387.

Di DW, Wu L, Zhang L, An CW, Zhang TZ, Luo P, Gao HH, Kriechbaumer V, Guo GQ. 2016a. Functional roles of Arabidopsis *CKRC2/YUCCA8* gene and the involvement of PIF4 in the regulation of auxin biosynthesis by cytokinin. *Scientific Reports* **6**: 36866.

Di DW, Zhang C, Luo P, An CW, Guo GQ. 2016b. The biosynthesis of auxin: how many paths truly lead to IAA? *Plant Growth Regulation* **78**: 275–285.

Ding ZJ, Yan JY, Xu XY, Li GX, Zheng SJ. 2013. WRKY46 functions as a transcriptional repressor of *ALMT1*, regulating aluminum-induced malate secretion in Arabidopsis. *The Plant Journal* **76**: 825–835.

Ding ZJ, Yan JY, Li CX, Li GX, Wu YR, Zheng SJ. 2015. Transcription factor WRKY46 modulates the development of Arabidopsis lateral roots in osmotic/salt stress conditions via regulation of ABA signaling and auxin homeostasis. *The Plant Journal* **84**: 56–69.

Enders TA, Strader LC. 2015. Auxin activity: past, present, and future. *American Journal of Botany* **102**: 180–196.

Glass AD, Britto DT, Kaiser BN, Kinghorn JR, Kronzucker HJ, Kumar A, Okamoto M, Rawat S, Siddiqi MY, Unkles SE *et al.* 2002. The regulation of nitrate and ammonium transport systems in plants. *Journal of Experimental Botany* **53**: 855–864.

Han X, Kumar D, Chen H, Wu S, Kim JY. 2014. Transcription factor-mediated cell-to-cell signalling in plants. *Journal of Experimental Botany* **65**: 1737–1749.

He W, Brumos J, Li H, Ji Y, Ke M, Gong X, Zeng Q, Li W, Zhang X, An F *et al.* 2011. A small-molecule screen identifies L-kynurenine as a competitive inhibitor of taa1/tar activity in ethylene-directed auxin biosynthesis and root growth in arabidopsis. *Plant Cell* **23**: 3944–3960.

Hoeberichts FA, Vaeck E, Kiddle G, Coppens E, van de Cotte B, Adamantidis A, Ormenese S, Foyer CH, Zabeau M, Inzé D *et al.* 2008. A temperature-sensitive mutation in the *Arabidopsis thaliana* phosphomannomutase gene disrupts protein glycosylation and triggers cell death. *Journal of Biological Chemistry* **283**: 5708–5718.

Hu Y, Dong Q, Yu D. 2012. Arabidopsis WRKY46 coordinates with WRKY70 and WRKY53 in basal resistance against pathogen *Pseudomonas syringae*. *Plant Science* **185–186**: 288–297.

Jadid N, Mialoundama AS, Heintz D, Ayoub D, Erhardt M, Mutterer J, Meyer D, Alioua A, Van Dorsselaer A, Rahier A *et al.* 2011. DOLICHOL PHOSPHATE MANNOSE SYNTHASE1 mediates the biogenesis of isoprenyl-linked glycans and influences development, stress response, and ammonium hypersensitivity in Arabidopsis. *Plant Cell* **23**: 1985–2005.

Jiao Q, Chen T, Niu G, Zhang H, Zhou CF, Hong Z. 2020. *N*-glycosylation is involved in stomatal development by modulating the release of active abscisic acid and auxin in Arabidopsis. *Journal of Experimental Botany* **71**: 5865–5879.

Kempinski CF, Haffar R, Barth C. 2011. Toward the mechanism of NH_4^+ sensitivity mediated by Arabidopsis GDP-mannose pyrophosphorylase. *Plant, Cell & Environment* **34**: 847–858.

Konishi N, Ishiyama K, Beier MP, Inoue E, Kanno K, Yamaya T, Takahashi H, Kojima S. 2017. Contribution of two glutamine synthetase isozymes to ammonium assimilation in Arabidopsis roots. *Journal of Experimental Botany* **68**: 613–625.

Korasick DA, Enders TA, Strader LC. 2013. Auxin biosynthesis and storage forms. *Journal of Experimental Botany* **64**: 2541–2555.

Kronzucker HJ, Britto DT, Davenport RJ, Tester M. 2001. Ammonium toxicity and the real cost of transport. *Trends in Plant Science* **6**: 335–337.

Kronzucker HJ, Siddiqi MY, Glass A. 1995. Analysis of $^{13}NH_4^+$ efflux in spruce roots (a test case for phase identification in compartmental analysis). *Plant Physiology* **109**: 481–490.

Kudoyarova GR, Farkhutdinov RG, Veselov SY. 1997. Comparison of the effects of nitrate and ammonium forms of nitrogen on auxin content in roots and the growth of plants under different temperature conditions. *Plant Growth Regulation* **23**: 207–208.

Li BH, Li GJ, Kronzucker HJ, Baluska F, Shi WM. 2014. Ammonium stress in Arabidopsis: signaling, genetic loci, and physiological targets. *Trends in Plant Science* **19**: 107–114.

Li BH, Li Q, Su YH, Chen H, Xiong LM, Mi GH, Kronzucker HJ, Shi WM. 2011. Shoot-supplied ammonium targets the root auxin influx carrier AUX1 and inhibits lateral root emergence in Arabidopsis. *Plant, Cell & Environment* **34**: 933–946.

Li B, Li Q, Xiong L, Kronzucker HJ, Krämer U, Shi W. 2012. Arabidopsis plastid metalloprotease AMOS1/EGY1 integrates with ABA signaling to regulate global gene expression in response to ammonium stress. *Plant Physiology* **160**: 2040–2051.

Li GZ, Wang ZQ, Yokosho K, Ding B, Fan W, Gong QQ, Li GX, Wu YR, Yang JL, Ma JF *et al.* 2018. Transcription factor WRKY22 promotes aluminum tolerance via activation of OsFRDL4 expression and enhancement of citrate secretion in rice (*Oryza sativa*). *New Phytologist* **219**: 149–162.

Li Q, Li BH, Kronzucker HJ, Shi WM. 2010. Root growth inhibition by NH_4^+ in Arabidopsis is mediated by the root tip and is linked to NH_4^+ efflux and GMPase activity. *Plant, Cell & Environment* **33**: 1529–1542.

Liu Y, Lai NW, Gao K, Chen FJ, Yuan LX, Mi GH. 2013. Ammonium inhibits primary root growth by reducing the length of meristem and elongation zone and decreasing elemental expansion rate in the root apex in *Arabidopsis thaliana*. *PLoS ONE* **8**: e60131.

Liu Y, von Wiren N. 2017. Ammonium as a signal for physiological and morphological responses in plants. *Journal of Experimental Botany* **68**: 2581–2592.

Lukowitz W, Nickle TC, Meinke DW, Last RL, Conklin PL, Somerville CR. 2001. Arabidopsis *cyt1* mutants are deficient in a mannose-1-phosphate guanylyltransferase and point to a requirement of N-linked glycosylation for cellulose biosynthesis. *Proceedings of the National Academy of Sciences, USA* **98**: 2262–2267.

Maruta T, Yonemitsu M, Yabuta Y, Tamoi M, Ishikawa T, Shigeoka S. 2008. Arabidopsis phosphomannose isomerase 1, but not phosphomannose isomerase 2, is essential for ascorbic acid biosynthesis. *Journal of Biological Chemistry* **283**: 28842–28851.

Michniewicz M, Zago MK, Abas L, Weijers D, Schweighofer A, Meskiene I, Heisler MG, Ohno C, Zhang J, Huang F *et al.* 2007. Antagonistic regulation of PIN phosphorylation by PP2A and PINOID directs auxin flux. *Cell* **130**: 1044–1056.

Munns R, Day DA, Fricke W, Watt M, Arsova B, Barkla BJ, Bose J, Byrt CS, Chen Z-H, Foster KJ *et al.* 2020. Energy costs of salt tolerance in crop plants. *New Phytologist* **225**: 1072–1090.

Qin C, Qian W, Wang W, Wu Y, Yu C, Jiang X, Wang D, Wu P. 2008. GDP-mannose pyrophosphorylase is a genetic determinant of ammonium sensitivity in *Arabidopsis thaliana*. *Proceedings of the National Academy of Sciences, USA* **105**: 18308–18313.

Rayle DL, Evans ML, Hertel R. 1970. Action of auxin on cell elongation. *Proceedings of the National Academy of Sciences, USA* **65**: 184–191.

Ren H, Lin D. 2014. ROP GTPase regulation of auxin transport in Arabidopsis. *Molecular Plant* **8**: 193–195.

Riechmann JL, Ratcliffe OJ. 2000. A genomic perspective on plant transcription factors. *Current Opinion in Plant Biology* **3**: 423–434.

Ron D, Walter P. 2007. Signal integration in the endoplasmic reticulum unfolded protein response. *Nature Reviews Molecular Cell Biology* **8**: 519–529.

Ruiz-May E, Hucko S, Howe KJ, Zhang S, Sherwood RW, Thannhauser TW, Rose JK. 2014. A comparative study of lectin affinity based plant N-glycoproteome profiling using tomato fruit as a model. *Molecular and Cellular Proteomics* **13**: 566–579.

Shen H, Chen J, Wang Z, Yang C, Sasaki T, Yamamoto Y, Matsumoto H, Yan X. 2006. Root plasma membrane H^+-ATPase is involved in the adaptation of soybean to phosphorus starvation. *Journal of Experimental Botany* **57**: 1353–1362.

Strasser R, Altmann F, Mach L, Glössl J, Steinkellner H. 2004. Generation of *Arabidopsis thaliana* plants with complex N-glycans lacking β1,2-linked xylose and core α1,3-linked fucose. *FEBS Letters* **561**: 132–136.

Straub T, Ludewig U, Neuhauser B. 2017. The kinase CIPK23 inhibits ammonium transport in *Arabidopsis thaliana*. *Plant Cell* **29**: 409–422.

Sun L, Di DW, Li G, Li Y, Kronzucker HJ, Shi W. 2020. Transcriptome analysis of rice (*Oryza sativa* L.) in response to ammonium resupply reveals the involvement of phytohormone signaling and the transcription factor OsJAZ9 in reprogramming of nitrogen uptake and metabolism. *Journal of Plant Physiology* **246–247**: 153137.

Swarup R, Bhosale R. 2019. Developmental roles of AUX1/LAX auxin influx carriers in plants. *Frontiers in Plant Science* **10**: 1306.

Takahashi K, Hayashi K, Kinoshita T. 2012. Auxin activates the plasma membrane H^+-ATPase by phosphorylation during hypocotyl elongation in Arabidopsis. *Plant Physiology* **159**: 632–641.

Tamura W, Hidaka Y, Tabuchi M, Kojima S, Hayakawa T, Sato T, Obara M, Kojima M, Sakakibara H, Yamaya T. 2010. Reverse genetics approach to characterize a function of NADH-glutamate synthase1 in rice plants. *Amino Acids* **39**: 1003–1012.

Tanaka H, Maruta T, Ogawa T, Tanabe N, Tamoi M, Yoshimura K, Shigeoka S. 2015. Identification and characterization of Arabidopsis AtNUDX9 as a GDP-d-mannose pyrophosphohydrolase: its involvement in root growth inhibition in response to ammonium. *Journal of Experimental Botany* **66**: 5797–5808.

Wang P, Yu W, Zhang J, Rengel Z, Xu J, Han Q, Chen L, Li K, Yu Y, Chen Q. 2016. Auxin enhances aluminium-induced citrate exudation through upregulation of *GmMATE* and activation of the plasma membrane H^+-ATPase in soybean roots. *Annuals of Botany* **118**: 933–940.

von Wiren N, Gazzarrini S, Gojon A, Frommer WB. 2000. The molecular physiology of ammonium uptake and retrieval. *Current Opinion in Plant Biology* **3**: 254–261.

Xia Y, Ma Z, Qiu M, Guo B, Zhang Q, Jiang H, Zhang B, Lin Y, Xuan M, Sun L *et al.* 2020. N-glycosylation shields *Phytophthora sojae* apoplastic effector PsXEG1 from a specific host aspartic protease. *Proceedings of the National Academy of Sciences, USA* **117**: 27685–27693.

Xuan YH, Priatama RA, Huang J, Je BI, Liu JM, Park SJ, Piao HL, Son DY, Lee JJ, Park SH *et al.* 2013. Indeterminate domain 10 regulates ammonium-mediated gene expression in rice roots. *New Phytologist* **197**: 791–804.

Yin H, Li M, Lv M, Hepworth SR, Li D, Ma C, Li J, Wang SM. 2020. SAUR15 promotes lateral and adventitious root development via activating H^+-ATPases and auxin biosynthesis. *Plant Physiology* **184**: 837–851.

Zeng W, Ford KL, Bacic A, Heazlewood JL. 2018. N-linked glycan micro-heterogeneity in glycoproteins of Arabidopsis. *Molecular and Cellular Proteomics* **17**: 413–421.

Zheng X, He K, Kleist T, Chen F, Luan S. 2015. Anion channel SLAH3 functions in nitrate-dependent alleviation of ammonium toxicity in Arabidopsis. *Plant, Cell & Environment* **38**: 474–486.

Supporting Information

Additional Supporting Information may be found online in the Supporting Information section at the end of the article.

Fig. S1 WRKY46 is involved in the response to high-ammonium (NH_4^+) stress.

Fig. S2 *wrky46-1* exhibits a similar high-NH_4^+ sensitivity to *wrky46*.

Fig. S3 Protein N-glycosylation mutations are linked to NH_4^+ sensitivity.

Fig. S4 *nudx9-KO* exhibits an increased high-NH_4^+ tolerance compared to *nudx9*.

Fig. S5 *wrky46-1* exhibits decreased N-glycoproteins compared to Col.

Fig. S6 Exogenous indole-3-acetic acid (IAA) can partially rescue high-NH_4^+-induced root growth inhibition.

Fig. S7 Transcription levels of IAA-conjugating genes in Col and WRKY46ox.

Fig. S8 Different abiotic stresses induce the transcription and expression of WRKY46.

Fig. S9 The W-box is not the key motif in the high-NH_4^+ response.

Fig. S10 Indole-3-acetic acid inhibits the transcription and expression of WRKY46.

Table S1 Primers used in this study.

Table S2 Transcription factors (Col-N vs Col) identified by RNA-seq.

Methods S1 β-glucuronidase (GUS) assay in Arabidopsis and *Nicotiana benthamiana*.

Methods S2 Quantitative real-time polymerase chain reaction (qRT-PCR) assay.

Methods S3 Liquid chromatography-tandem mass spectrometry (LC-MS/MS) determination of free IAA and IAA conjugates.

Methods S4 Yeast one-hybrid (Y1H) assay.

Please note: Wiley Blackwell are not responsible for the content or functionality of any Supporting Information supplied by the authors. Any queries (other than missing material) should be directed to the *New Phytologist* Central Office.